

**Machine learning algorithms-based evaluation of dynamic properties and  
liquefaction potential of soil**



By

**Muhammad Abdul Mueed**

(Registration No: 326905)

Department of Geotechnical Engineering

NUST Institute of Civil Engineering

School of Civil and Environmental Engineering

National University of Sciences & Technology (NUST)

Islamabad, Pakistan

(2024)

**Machine learning algorithms-based evaluation of dynamic properties and  
liquefaction potential of soil**



By

**Muhammad Abdul Mueed**

(Registration No: 326905)

A thesis submitted to the National University of Sciences and Technology, Islamabad, in partial

fulfillment of the requirements for the degree of

**Master of Science in Geotechnical Engineering**

Thesis Supervisor: **Dr. Tariq Mahmood Bajwa**

NUST Institute of Civil Engineering

School of Civil and Environmental Engineering


National University of Sciences & Technology (NUST) Islamabad, Pakistan

# THESIS ACCEPTANCE CERTIFICATE

Photo is attached


## THESIS ACCEPTANCE CERTIFICATE

It is certified that final copy of MS thesis written by Mr. Muhammad Abdul Mueed (Registration No. NUST-2020-MS-Geotech-00000326905) of NUST INSTITUTE OF CIVIL ENGINEERING (NICE), has been vetted by undersigned, founded complete in all respects as per NUST Statutes / Regulations, free of plagiarism, errors, and mistakes and is accepted as partial fulfillment for the award of MS degree. It is further certified that necessary amendments as pointed out by GEC members of the scholar have also been incorporated in the said thesis.

Signature:  08/7/2024  
Supervisor: Dr. Tariq Mahmood Bajwa  
Date: July 08, 2024

Signature:   
Head of Department: Dr. Badar Al-Shameri  
Date:   
Head Geotechnical Engineering  
NIST Institute of Civil Engineering  
School of Civil & Environmental Engineering  
National University of Sciences and Technology

Signature:  ✓  
Associate Dean: Dr. S. Muhammad Jamil  
Date: July 10, 2024  
Dr. S. Muhammad Jamil  
Associate Dean  
NICE, SCEE, MUST

Signature:   
Principal & Dean (SCEE-NICE): Prof. Dr. Muhammad Irfan  
Date: 10 JUL 2024  
PROF DR MUHAMMAD IRFAN  
Principal & Dean  
SCEE, MUST

**ATTACH A COPY OF TH-4 FORM**

Form TH-4

**National University of Sciences and Technology**  
**MASTER'S THESIS WORK**

We hereby recommend that the dissertation prepared under our Supervision by: **Muhammad Abdul Mueed**, Regn No. **00000326905**  
Titled: **“Machine Learning Algorithms Based Evaluation of Dynamic Properties and Liquefaction Potential of Soil”** be accepted in partial fulfillment of the requirements for the award of degree with B+ Grade

**Examination Committee Members**

1. Name: Dr. S. Muhammad Jamil

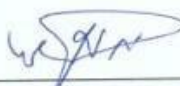
Signature: \_\_\_\_\_ ✓

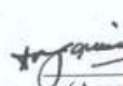
2. Name: Dr. Azam Khan

Signature: \_\_\_\_\_

Supervisor's name: Dr. Tariq Mahmood Bajwa

Signature: \_\_\_\_\_


  
Head of Department  
HoD Geotechnical Engineering  
NUST Institute of Civil Engineering  
School of Civil & Environmental Engineering  
National University of Sciences and Technology

  
Dr. S. Muhammad Jamil  
Associate Dean  
(Associate Dean)  
NICE, SCEE, NUST

*Sir, 5x pages,  
please.*

**COUNTERSIGNED**

Date: 10 JUL 2024

  
Principal & Dean SCEE  
PROF DR MUHAMMAD IRFAN  
Principal & Dean  
SCEE, NUST

# CERTIFICATE OF APPROVAL

Photo is attached

## Certificate of Approval

This is to certify that the research work presented in this thesis, entitled "Machine Learning Algorithms Based Evaluation of Dynamic Properties and Liquefaction Potential of Soil" was conducted by Mr. Muhammad Abdul Mueed under the supervision of Dr. Tariq Mahmood Bajwa.

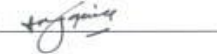
No part of this thesis has been submitted anywhere else for any other degree. This thesis is submitted to the National University of Sciences and Technology (NUST) in partial fulfillment of the requirements for the degree of Master of Science in field of Geotechnical Engineering from NUST institute of Civil Engineering (NICE), School of Civil and Environmental Engineering (SCEE), NUST

Student Name: Muhammad Abdul Mueed

Signature:  <sup>md.</sup>

Examination Committee:

a) GEC Member 1: Dr. S. Muhammad Jamil

Signature: 

b) GEC Member 2: Dr. Azam Khan

Signature: 

Supervisor: Dr. Tariq Mahmood Bajwa

Signature:  08/1-7/2024


HOD: Dr. Badee Alshameri

Signature:   
HoD Geotechnical Engineering  
NICE, SCEE, NUST

Associate Dean: Dr. S. Muhammad Jamil

Signature:   
Dr. S. Muhammad Jamil  
Associate Dean  
NICE, SCEE, NUST

Principal & Dean: Prof. Dr. Muhammad Irfan

Signature:   
PROF. DR. MUHAMMAD IRFAN  
Principal & Dean  
SCEE, NUST

## Author's Declaration

Photo is attached.

### Author's Declaration

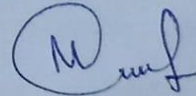
I Muhammad Abdul Mueed, hereby state that my MS thesis titled

“Machine Learning Algorithms Based Evaluation of Dynamic Properties and Liquefaction Potential of Soil”

is my own work and has not been submitted previously by me for taking any degree from this University **National University of Sciences & Technology, NUST Islamabad**, or anywhere else in the country/world.

At any time if my statement is found to be incorrect even after I graduate the university has the right to withdrawn my MS Degree.

Signature:



Name of Student: Muhammad Abdul Mueed

Dated: 08/07/2024

# PLAGIARISM UNDERTAKING

Photo is attached



## CERTIFICATE FOR PLAGIARISM

It is certified that MS Thesis Titled “Machine Learning Algorithms Based Evaluation of Dynamic Properties and Liquefaction Potential of Soil” by Regn No. 00000326905, Muhammad Abdul Mueed has been examined by us. We undertake the follows:-

- a. Thesis has significant new work/knowledge as compared already published or are under consideration to be published elsewhere. No sentence, Equation, table, paragraph or section has been copied verbatim from previous work unless it is placed under quotation marks and duly referenced.
- b. The work presented is original and own work of the author (i.e. there is no plagiarism). No ideas, processes, results, or words of others have been presented as author own work.
- c. There is no fabrication of data or results which have been compiled / analyzed.
- d. There is no fabrication by manipulating research materials, equipment, or processes, or changing or omitting data or results such that the research is not accurately represented in the research record.
- e. The thesis has been checked using TURNITIN (copy of originality report attached) and found within limits as per HEC Plagiarism Policy and instructions issued from time to time.

Signature: \_\_\_\_\_

*Tariq Mahmood Bajwa* 08/07/2024

Name of Supervisor: Dr. Tariq Mahmood Bajwa

**DEDICATED**  
**To**  
**MY FATHER & MOTHER**



## **ACKNOWLEDGEMENTS**

All praise to Almighty Allah, who gave me the courage and power to complete this research work and gratitude to the last Prophet MUHAMMAD (P.B.U.H).

I extend my wholehearted gratitude to my revered supervisor, Dr. Tariq Mahmood Bajwa, for his technical guidance, indelible help and valuable feedback throughout this study. I also express my utmost gratitude to GEC members Dr. Syed Muhammad Jamil and Dr. Azam Khan for providing helpful feedback on various aspects of this study from time to time.

I would like to acknowledge my brother Muhammad Abdul Aleem and colleagues Syed Jamal Arbi, Muhammad Shahroz Khalid, Rashid Gabool, Zeeshan Khurshid, Hafiz Muhammad Asif and Ghulam Abbas for their support and for making my stay at NUST pleasant and memorable.

## ABSTRACT

Machine learning models are the viable option contrary to the conventional experimental procedures that are complicated and tedious for liquefaction potential prediction. This study leverages the strength of machine learning models including K-nearest neighbor (KNN), random forest (RF), gradient boost (GB), extreme gradient boost (XGB), decision tree (DT) and artificial neural network (ANN) for predicting the soil responses and liquefaction susceptibility by utilizing the 500 SPT-N cases as input dataset. The predictive capabilities of models in assessing the intricate relationship between various soils parameters are assessed by employing the evaluation matrices of mean squared error (MSE), root mean square error (RMSE), mean absolute error (MAE), Nash-Sutcliffe efficiency, Percent Bias, Weighted Index and R2. Moreover, the comparative analysis of the models has been conducted to find the best optimized model for liquefaction potential determination by accuracy matrix, Akaike information criterion (AIC) and ranking analysis. The results indicated that RF model exhibited the highest prediction efficiency for shear stress with R2 of 0.998. Similarly, GB indicated the better performance as compared to other models in evaluating the shear wave velocity with 0.992 coefficient of determination (R2). The most important and critical parameter for liquefaction maximum shear modulus ( $G_{max}$ ) is predicted with high accuracy by all models with outperformance of ANN having R2 value of 0.999. Moreover, liquefaction potential index (LPI) is also well predicted by XGBoost model. The performance trend of all the models for each of the parameters is also in accordance with AIC criteria. Furthermore, scaling analysis of all models for collective comparison put RF model on rank first for overall prediction of liquefaction potential and dynamic properties. XGBoost and DT showed second and third best performance, followed by GB as fourth, ANN as fifth and KNN as least effective model for this task. The findings of this study offer sophisticated models for evaluating soil behavior and liquefaction potential, which has important ramifications for geotechnical engineering.

**Keywords:** Machine Learning (ML), Dynamic properties, Liquefaction potential, DEEPSOIL, SPT-N dataset

# TABLE OF CONTENTS

ABSTRACT.....	i
LIST OF FIGURES .....	v
LIST OF TABLES .....	vi
LIST OF ACRONYMS.....	1
1 Chapter 1: Introduction.....	1
1.1 General .....	1
1.1.1 Soil dynamics Properties.....	2
1.1.2 Machine learning .....	3
1.1.3 Machine learning approaches .....	3
1.1.4 Research Gap .....	4
1.2 Significance of Research.....	5
1.3 Scope of Research .....	6
1.4 Objective of the research work.....	6
1.5 Scheme of chapters.....	6
2 Chapter 2: Literature Review .....	8
2.1 General .....	8
2.2 Soil Liquefaction.....	8
2.3 Earthquake and Soil Dynamics effects on Construction industry.....	9
2.4 SPT-N count (N).....	10
2.5 Shear wave velocity ( $V_s$ ) .....	11
2.6 Maximum Shear Modulus ( $G_{max}$ ).....	12
2.7 Shear Stress ( $\tau$ ).....	13
2.8 Liquefaction Potential Index (LPI) .....	15
2.9 Overview of Machine Learning .....	16
2.9.1 K-Nearest Neighbors (KNN).....	17
2.9.2 Random Forest Algorithm.....	18
2.9.3 Support Vector Regression (SVR) .....	18
2.9.4 XGBoost Algorithm .....	19
2.9.5 Decision Tree .....	20

2.9.6	Gradient Boost .....	21
2.9.7	Artificial Neural Network.....	21
2.10	Model Evaluation Metrics.....	23
3	Chapter 3: Methodology.....	24
3.1	Study area.....	25
3.2	Soil Profile.....	27
3.3	Data Collection.....	28
3.4	Data screening.....	29
3.5	Removing Outlier:.....	29
3.6	Data Partition: .....	31
3.7	Experimental Setup .....	31
3.8	Architecture of Models.....	32
3.8.1	K-Nearest Neighbors (KNN) .....	32
3.8.2	Random Forest (RF) .....	33
3.8.3	Gradient Boosting (GB).....	33
3.9	Extreme Gradient Boosting (XGBoost).....	34
3.9.1	Decision Trees (DT).....	35
3.10	Artificial Neural Network (ANN).....	35
3.11	Performance Evaluation:.....	36
4	Chapter 4: Results and discussion .....	38
4.1	Preprocessed data .....	38
4.1.1	Soil Parameters Analysis.....	38
4.1.2	Graphical Representation of Actual and Predicted Values .....	39
4.1.3	Shear Stress.....	39
4.1.4	Shear wave Velocity.....	42
4.2	Maximum Shear Modulus.....	43
4.3	Liquefaction Potential Index .....	46
4.4	Performance analysis.....	48
4.4.1	Accuracy Matrix .....	50
4.4.2	AIC Criteria .....	53
4.5	Rank Analysis.....	55

5	Chapter 5: Conclusions.....	57
6	References .....	59

## LIST OF FIGURES

Figure 1.1: Dynamic load test and static load test at the site.....	1
Figure 1.2: Soil dynamics and earthquake.....	5
Figure 1.3: Scheme of chapters.....	7
Figure 2.1: K-Nearest Neighbors prediction model architecture.....	17
Figure 2.2: Random Forest prediction model architecture.....	18
Figure 2.3: Support vector machine model architecture.....	19
Figure 2.4: Extreme Gradient Boost prediction model architecture.....	20
Figure 2.5: Gradient Boost prediction model architecture.....	21
Figure 2.6: ANN prediction model architecture.....	22
Figure 3.1: Methodology flow charts.....	25
Figure 3.2: Study area map.....	27
Figure 3.3:K-Neighbors prediction model code.....	32
Figure 3.4: Random Forest prediction model code.....	33
Figure 3.5: Gradient Boost prediction model code.....	34
Figure 3.6: Extreme Gradient Boost prediction model code.....	34
Figure 3.7: Decision Tree prediction model code.....	35
Figure 3.8: ANN prediction model code.....	36
Figure 4.1 : Scatter graphs for shear stress prediction: (a) KNN, (b) RF, (c) GB, (d) XGBoost, (e) DT and (f) ANN.....	41
Figure 4.2: Scatter graphs for shear wave velocity prediction: (a) KNN, (b) RF, (c) GB, (d) XGBoost, (e) DT and (f) ANN.....	43
Figure 4.3: Scatter graphs for shear wave velocity prediction: (a) KNN, (b) RF, (c) GB, (d) XGBoost, (e) DT and (f) ANN.....	45
Figure 4.4: Scatter graphs for LIP prediction: (a) KNN, (b) RF, (c) GB, (d) XGBoost, (e) DT and (f) ANN.....	47
Figure 4.5: Accuracy Matrix of statistical parameters data (a) SS (b) SV (c) Gmax (d) LPI.....	52
Figure 4.6: Illustration of all proposed Model's AIC values using Radar Diagram for (a) SS parameter (b) SV parameter (c) Gmax parameter.....	55

## LIST OF TABLES

Table 3.1: Introduction of input parameters.....	29
Table 3.2: Statistical dataset.....	30
Table 4.1: Performance Matrices values for all models.....	48
Table 4.2 AIC values of parameters for all proposed models .....	53
Table 4.3: Ranking analysis of all models for dynamic properties and liquefaction potential determination .....	56

## LIST OF ACRONYMS

No.	Abbreviations	Description
1	ML	Machine Learning
2	SVR	Support Vector Regression
3	RF	Random Forest
6	ANN	Artificial Neural Network
7	DT	Decision Tree
8	XGBOOST	Extreme Gradient Goosing
9	SD	Soil Dynamics
10	RMSE	Root Mean Square Error
11	$R^2$	Coefficient of Determination
12	MAE	Mean Absolute Error
13	SPT	Standard Penetration Test
14	SS	Shear Stress
15	SWV	Shear wave velocity
16	LPI	Liquefaction Potential Index



# Chapter 1: Introduction

## 1.1 General

Soil liquefaction is a complex phenomenon observed in several earthquakes in various forms. Upon liquefaction of a soil deposit, excess pore pressures within the soil reach the effective stress level, causing significant reduction in resilience and stiffness. Effects such as excessive settlements, tilting, and lateral movement can be observed during and after an earthquake. These effects mostly cause large-scale destruction of life and structures. A soil's susceptibility to liquefaction is influenced by several variables, including its type, density, saturation level, and the intensity and frequency of vibrations during a seismic event. Understanding these variables and their interplay is essential for assessing an area's susceptibility to liquefaction and developing suitable countermeasures (Guo, Zhuang, Chen, & Zhu, 2022).



**Figure 1.1:** Dynamic load test and static load test at the site

The primary cause of soil dynamics is loss of soil shear strength, resulting from an increase in pore pressure (Zheng et al., 2024). Before undertaking large-scale projects, a thorough evaluation of the liquefaction potential in the seismically active area surrounding the dam site must be conducted to minimize risks of failure. Evaluating liquefaction potential is also crucial before implementing prevention and mitigation strategies. Therefore, accurate prediction of soil liquefaction is

paramount in geotechnical engineering. Over the past decade, considerable research has employed machine learning (ML) techniques to forecast soil liquefaction. 'Dynamic properties' refer to how soil responds to dynamic loading, such as vibrations or earthquakes. Shear modulus, damping ratio, and wave propagation properties are some of these characteristics (Zeng et al., 2024).

### **1.1.1 Soil dynamics Properties**

Shear wave velocity ( $V_s$ ) analysis is a vital method for assessing the soil's susceptibility to liquefaction. One crucial factor that reveals the strength and stiffness properties of the material is the soil's shear wave velocity, which also indicates its fluidity. This information is crucial for understanding how the soil responds during earthquakes. A shear wave velocity test generates seismic waves that propagate through the soil (Mondal & Kumar, 2024). The test typically involves placing seismic sensors such as accelerometers or geophones at various depths in the soil profile. Seismic generators, such as hammer strikes or seismic vibrators, mechanically induce vibrations into the soil. Factors such as soil type, density, moisture content, and stress conditions influence shear wave velocity. Stiffer, denser soils with higher shear wave velocities generally exhibit greater resistance to earthquake shaking and lower liquefaction risk. Conversely, loose, low-density soils often show lower shear wave velocities, indicating weaker stiffness and higher liquefaction susceptibility.

Increased pore pressure due to cyclic loading during seismic events can occur from dynamic soil reactivity. The soil's properties and drainage characteristics determine the depth at which excess pore water pressure dissipates. Accumulated pore water pressure is critical in assessing liquefaction potential, influenced by factors such as soil porosity, groundwater conditions, and the presence of confining layers. In-situ or laboratory studies are commonly used to assess how pore water pressure changes with depth (Bhalawe et al., 2024).

The dynamic shear modulus, represented as  $G$ , is a key measure of a soil's stiffness under cyclic or dynamic loading conditions. It is crucial for understanding how well the soil can resist shear deformations under seismic forces. The dynamic modulus of elasticity typically depends on frequency, indicating that the applied force velocity can affect its value. With increasing strain levels, the maximum shear modulus ( $G_{max}$ ) decreases, indicating reduced stiffness under larger loads. Soil aging and degradation can also impact  $G_{max}$ , affecting the soil's ability to resist shear

deformations. Understanding  $G_{max}$  provides valuable insights into soil stiffness and its performance under dynamic stresses such as earthquakes. This knowledge aids in the design and evaluation of structures for stability and performance during seismic events (Pakzad & Arduino, 2024)

### **1.1.2 Machine learning**

Machine learning algorithms have gained a lot of attention recently due to their efficaciousness as instruments for result prediction and sophisticated data analysis across a range of industries, including geotechnical construction. Using large-scale datasets and the deciphering of complex relationships between the properties of soil and seismic activity, machine learning algorithms offer a viable way to improve our understanding and prediction of the dynamic properties and liquefaction capacity of soil. An effective method for gaining knowledge about the properties of subsurface soil is the SPT-N test. Taking several SPT-N measurements at different depths allows for the identification of soil layering, changes in soil properties, and variations in liquefaction vulnerabilities within the soil profile. This information makes it easier to characterize the site, allowing engineers to assess the likelihood of liquefaction's geographical distribution and modify mitigation plans as needed (Padarian, Minasny, & McBratney, 2020).

### **1.1.3 Machine learning approaches**

In geotechnical engineering, a variety of machine learning models, including supported vector machines, random forest neural network models, and Gradient Boosting Machines, have been used to estimate shear modulus. These algorithms provide useful tools for precise prediction by capturing intricate correlations between the input parameters and soil variables. The kind of data and the degree of precision needed for a given application determine which model is best. The damping ratio significantly influences soil dynamics during seismic events. A higher damping ratio allows the soil to dissipate more energy, reducing the amplitude of vibrations and mitigating potential damage to structures. It affects settlement behavior, especially in loose and liquefiable soils, impacting the susceptibility to liquefaction-induced damage (Ozsagir, Erden, Bol, Sert, & Özocak, 2022). Accurate estimation of damping ratio is vital for soil-structure interaction analysis and seismic hazard assessment, ensuring resilient engineering design and risk evaluation. Different machine learning algorithms predict damping ratios in soil dynamics by analyzing historical data on soil behavior under dynamic loading. These models capture complex relationships between

input parameters and damping ratios, providing accurate predictions for seismic response analysis. Various approaches have been applied in the literature for assessing the liquefaction potential of soil. XGBoost- SHAP model proposed by Jas et al. indicated the prediction efficiency of 88.24 % for liquefaction potential evaluation. Various models have been suggested by (Ozsagir, Erden, Bol, Sert, & Özocak, 2022) for assessing the liquefaction of fine soil and found the DT model with 90 % success rate. ANN network was also proposed to identify the properties of liquefaction in Iran which indicated less than 5 % uncertainty. (Hanandeh et al. 2022) comparatively investigated three ML models including QDA, SVM and DT and found the highest precision of 0.94 and accuracy of 0.97 for QDA model in liquefaction identification. (Cai et al. 2022) utilized the LSSVM and RBFNN in combination with WGO, DE and GA for liquefaction potential studies. They found the better efficiency of WGO algorithm for optimizing both models. (Zhao et al. 2021) a hybrid machine learning algorithm based on PSO-KELM to evaluate the liquefaction by utilizing cone penetration test and shear wave velocity. It improved the liquefaction prediction accuracy by indicating  $R^2$  values of 0.839 and 0.892. (Kumar et al. 2023) also investigated the efficiency of DNN, CNN, RNN, LSTM and BILSTM for liquefaction prediction by employing the SPT-based data. RNN indicated the highest performance for N160 and CSR prediction and in return the liquefaction with  $R^2$  of 0.906 and 0.10 RMSE. Similarly various other studies also investigated the role of Machine learning models for liquefaction prediction like ANFIS-FF model by Ghani et al., ANN model, ANN-GP model, Greedy-AutoML and others.

#### **1.1.4 Research Gap**

This indicated that limited research has been conducted related to prediction of seismic soil liquefaction through Standard penetrations test. Conventional models are unable to determine both dynamic properties (Shear Modulus, Damping ratio, Shear wave velocity) along with liquefaction potential of soil. In seismically active zones, machine learning has not been used to assess the dynamic response and growth of pore water pressure, particularly in the areas between the Chenab and Jhelum rivers. This research deals with a comparatively large dataset of soils and assessed by using deep-soil software. The objective of this research is to utilize the most obedient algorithm of machine learning for the predictions of shear stress, Maximum shear modulus, Shear wave velocity to predict the liquefaction potential of soil. The SPT-N data obtained from the study area by subsurface soil investigation has been utilized as input for ML models. Machine learning models serve as beneficial in determining the dynamic properties or liquefaction potential by considering

the parameters of PPW, Shear Stress, Shear Wave velocity, Dynamic ratio, LPI and Maximum shear modulus. These proposed models including KNN, RF, GB, XGBoost, DT and ANN vary in their performance in predicting the various parameters for liquefaction potential determination. The effectiveness of these models has been compared and the experimental findings indicated the viability of the suggested algorithms. The model's performance has been assessed by utilizing the evaluation matrices. Furthermore, performance matrices, AIC criteria, and scaling analysis have been conducted to compare their efficiency of prediction. These parameters help the researchers or academics to train the predictive models on this type of dataset that are highly accurate in determining the liquefaction potential or dynamic features. Better seismic risk assessments are made possible by these models, which help with the construction of resilient infrastructure and buildings in liquefaction-prone areas. Machine learning is a helpful tool for improving the reliability of geotechnical assessments and expanding our understanding of soil behavior under dynamic situations because of its capacity to handle complicated, multi-dimensional datasets.



**Figure 1.2:** Soil dynamics and earthquake

## **1.2 Significance of Research**

Soil properties are the most important parameters for the stability of soil and these impact our daily life. To analyze the natural geological phenomena and engineering projects, the evaluation of soil dynamic properties and liquefaction potential is considered compulsory. Moreover, continuously

increasing natural disasters affect the soil condition that should be known for the future and Machine Learning is considered an advanced technique for this purpose.

### **1.3 Scope of Research**

Soil response under various hydraulic conditions and natural phenomena is important for the stability of the soil therefore, it is our national need to determine the type of soil, its properties like density, pore pressure and liquefaction potential to tackle with the problems during water resources management, drinking water supply, slope stability, land slide and other subsurface and geological engineering problems. There is long-term change in soil properties due to natural disasters like earthquakes and flooding so, there must be proper study to cover them.

### **1.4 Objective of the research work**

The current study aims to utilize advanced ML algorithms - Random Forest, Artificial Neural Network (ANN), and XGBoost for the quick and economical prediction of dynamic properties and liquefaction potential index (LPI) using SPT-N value and shear wave velocity.

- 1) Calculation of liquefaction potential index using standardized correlations.
- 2) Use advanced machine learning methods: KNN, RF, ANN, GB, XGBoost, and DT
- 3) Implement a thorough strategy for model validation, ensuring clarity at every stage.
- 4) Utilize multiple evaluation techniques for comprehensive model assessment of best performance.

### **1.5 Scheme of chapters**

The details about the chapters are given below. The scheme of the chapters is also shown in Figure 1.2.

**Chapter. 1:** This chapter highlights the precise summary of the research work.

**Chapter. 2:** This chapter reports a literature review of liquefaction potential determination techniques, machine learning in geotechnical engineering, and previous research on SPT-N tests.

**Chapter. 3:** This chapter discusses research methods involved in the formulation of machine learning algorithms, and model evaluations, etc.

**Chapter. 4:** This chapter discusses the experimental setup to achieve the research objectives.

**Chapter. 4:** This chapter reports the results and discussions.

**Chapter. 5:** This chapter summarizes the conclusions and key recommendations from the study.

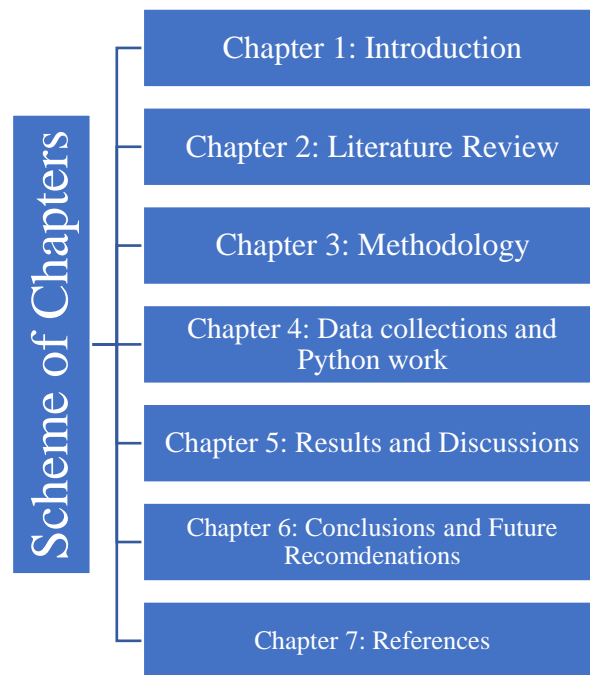


**Figure 1.3:** Scheme of chapters

## **Chapter 2: Literature Review**

### **2.1 General**

Liquefaction is considered a damaging phenomenon of earthquakes and a major cause of concern in civil engineering. Therefore, its predictor assessment is an essential task for geotechnical experts. Pakistan lies in a seismically active and earthquake prone region of the world where Indian, Eurasian, and Arabian plates are interacting at different rates of movement. This study investigates the performance of three machine learning algorithms Artificial neural network, Support vector machine and XGBoost algorithm depending upon different soil parameters. To evaluate the dynamic response and development of pore water pressure in seismically active zone of between Chenab and Jhelum River generalized/Hyperbolic constitutive model will be combining with PWP development model in a one-dimensional seismic site response to evaluate PWP development beneath the soil layer. The result shows the behavior of seismic soil based upon the attained model parameters of empirical equation. These three models will be trained through Mean square error; Mean absolute error, Mean Bias error and coefficient of determination. This study also interprets the probabilistic reasoning of the robust model and most probable explanation of seismic soil liquefied sites, based on an engineering point of view (Zhang, Yin, & Jin, 2022).

### **2.2 Soil Liquefaction**

One of the main factors contributing to building and structural instability during earthquakes is liquefaction, which makes it a crucial component of seismic research and foundation design. Almost every large earthquake causes widespread liquefaction-induced ground displacement and associated damage to soils and foundations, both of which have dramatic and disastrous effects. Liquefaction features may vary in geometry, type, and dimension at different locations because of multiple factors, including anomalous propagation and amplification of the seismic waves, and geological conditions (e.g., grain distribution and density of soil, groundwater level) (Galli 2000). A summary of the relationships and contrasts of liquefaction characteristics and related damage in previous earthquakes may help (1) to understand the mechanisms of liquefaction and (2) to develop hazard assessments for seismically induced liquefaction Piles transfer structural loads to stronger soil layers or rock strata deep below the surface. These elongated columns, commonly formed from materials like steel, concrete, or wood, are critical in supporting structures where surface soil



conditions are unsuitable for conventional shallow foundations. The selection of the foundation design depends upon the soil dynamics properties. During design there are different components chosen for it like soil types, site area, seismic location and ground water table. There are different types of foundations and have different characteristics (Khasawneh, Al-Akhrass, Rabab'ah, & Al-sugaier, 2024).

### **2.3 Earthquake and Soil Dynamics effects on Construction industry**

During building of seismic design liquefaction is a significant factor that's considered. Building foundations failure occurs due to when soil strength decreases. Soil strength decreases when the soil is saturated. The consequent displacement of the earth can seriously harm foundations and soil, endangering the structural integrity of buildings. Several large earthquakes are historical instances of liquefaction inflicting considerable destruction. Building collapses resulting from liquefaction and significant soil displacement were triggered by the 1964 Tokyo Earthquake in Japan. Like this, the devastating impacts of collapse on urban structures were brought to light by the Chinese Tangshan Earthquake of 1976 and the Taiwanese Chi-Chi Earthquake of 1999. In response to these incidents, engineers and academics have carried out extensive study to understand and mitigate this phenomenon (Luque & Bray, 2020). Engineers and academics want to improve their ability to anticipate, stop, and lessen the negative consequences of liquefaction on infrastructure and structures by studying these past examples. To make communities more resilient to seismic shocks, this study is crucial. Because of geological parameters such soil grain transportation, density, and groundwater level, as well as the transmission and intensification of seismic waves, liquefaction features can vary greatly in terms of geometry, kind, and size at different places (Arboleda-Monsalve, Mercado, Terzic, & Mackie, 2020). To understand liquefaction mechanisms and create risk assessments for earthquake-induced liquefaction, it is essential to appreciate the correlations and differences in liquefaction characteristics and the ensuing damage from prior earthquakes. Most of the recent research on liquefaction of soil from earthquakes in the twenty-first century has concentrated on incidents and has not thoroughly examined general characteristics and associated harm done to soil and buildings. Enhancing risk assessments and mitigation measures would require a more comprehensive examination of several recent occurrences to get a deeper comprehension of the macroscopic impacts of soil liquefaction (Mourlas et al., 2020).

## 2.4 SPT-N count (N)

In geotechnical engineering, the standard penetrating test (SPT) is frequently utilized to evaluate the characteristics of soil. By measuring soil barriers to penetration, the SPT-N count yields important details regarding the density, durability, and dynamic features of the soil. This investigates the connection between soil dynamics, SPT-N levels, and the likelihood of soil liquefaction. With the SPT, a regular hammer is used to drive a split-barrel sample into the ground at the lowest of a borehole. The N value is the total amount of blows needed to move the sampler a certain distance. As a measure of the behavior of the soil under dynamic as well as static loads, the N value is essential for determining the density and strength of the soil (Ayala, Sáez, & Magna-Verdugo, 2022). N values are used in soil dynamics, the study of soil behavior during cyclic or transient stresses, such as earthquakes to calculate soil stiffness & shear strength. Increased pressure within the pores causes saturated, loose, granular dirt to become more fluid and lose their strength and stiffness, resulting in soil liquefaction. When determining the soil's susceptibility to liquefaction, the SPT-N count is crucial. Based on lab research and field case studies, empirical connections between N levels and potential for liquefaction have been established. There are known critical N value limits below where soils are more prone to liquefied in the event of an earthquake. The distribution of grain sizes, confining tension, and soil type all affect these thresholds. In sands and silty sands, for example, low N fields are more susceptible to collapse than higher N soils (Kasim & Raheem, 2021). Simplified techniques for assessing liquefaction potential, such the Seed and Idriss approach, integrate these findings. These correlations' refinements consider further variables including fines content and overburden pressure. Readjusting the observed N value for pressure from overburden and hammer efficiency of energy yields a correct N value  $(N_1)_{60}$  that increases the accuracy of liquefaction forecast. To take into consideration the unpredictability and variety of soil qualities and seismic loading circumstances, probabilistic techniques have been devised. Integration of SPT data with geophysical and other in situ testing techniques is one of the recent advances. SPT-N values and shear wave velocity observations together offer a more thorough evaluation of soil flexibility and potential for liquefaction. The liquefaction hazard estimates are more reliable because to these combined methodologies. Developing regional liquefaction hazard maps using SPT data is another significant advancement, incorporating spatial variations in soil properties and seismic hazard levels to identify high-risk areas (Lu & Hwang, 2020). These maps are useful for disaster

preparedness, infrastructure design, and urban planning. Notwithstanding these developments, there are still issues with liquefaction evaluation using SPT data. Unpredictability in SPT protocols, apparatus, and operator methods can result in inconsistent N values. There is continuous work being done to enhance data quality and standardize SPT procedures. In geotechnical engineering, the SPT-N count is essential because it offers information on the density, strength, and dynamical behavior of the soil. Because of its function in determining the possibility for soil liquefaction, empirical correlations and streamlined liquefaction evaluation techniques have been developed. Understanding and forecasting liquefaction risks have improved by the integration of SPT data using other testing techniques and the creation of regional hazard maps. In order to increase the application and reliability of SPT-based liquefaction evaluations and create safer, more robust infrastructure in earthquake-prone locations, further research and standardization initiatives are needed (Yabe, Harada, Ito, & Watanabe, 2022).

## **2.5 Shear wave velocity ( $V_s$ )**

The assessment of the link between liquefaction of soil and velocity of shear waves is a critical aspect of geotechnical engineering. Shear wave velocity is a crucial metric for predicting the behavior of soils during seismic events, in addition to being used to assess the liquefaction potential of soils. Below is a summary of several important studies on the connection between land liquefaction with shear wave velocity (Yunmin, Han, & Ren-peng, 2005).

Various researchers have determined a connection between soil seismic sensitivity and shear wave velocity. They found that the shear wave velocity is a significant factor affecting how much the ground moves during earthquakes. the effect of soil properties on the connection between shear wave velocity and earthquake-induced ground motion. They found that the link between ground motion and shear wave velocity depended on soil type, water below the surface straight, and stress history. An innovative method of predicting the velocity of soil shear waves is through the use of machine learning algorithms. Using information from seismic surveys and lab experiments, they developed a model that can predict the velocity of soil shear waves depending on input parameters such as distribution of particle sizes and geology(Forte et al., 2019).

The study found a substantial correlation between shear wave velocity and earthquakes, indicating that shear wave velocity plays a critical role in regulating the behavior of soil during seismic events. Numerous methods, including algorithms for machine learning, seismic inquiries, and

laboratory testing methods, can be used to determine shear wave velocity. These methods are essential for constructing earthquake-resistant buildings as well as other fundamental uses. The velocity of waves caused by shear ( $V_s$ ) in non-cohesive soils is a crucial indicator of the likelihood of liquefaction. Since the 1980s, scientists have been able to identify connections between  $V_s$  and durability against liquefaction using data from both the lab and the field. These correlations can be directly obtained from measurements of  $V_s$ , such as seismic cone penetration tests (SCPT), or they can be deduced from a variety of in situ studies, such as the traditional penetration test (SPT-N) or a cone penetration test (CPT-qc) for liquefied places. Seed et al. were the first to propose a relationship between the cyclic resistant ratio (CRR) and standardized the velocity of shear waves ( $V_{s1}$ ), considering the relationship between SPT-N and  $V_s$ . In the early 1990s, several research developed  $V_{s1}$ -based resistance to liquefied correlations by directly determining  $V_s$  at liquefied places. Using these  $V_s$ -based patterns, engineers may improve the predictability and resilience of structures constructed on non-cohesive properties by lessening the risk of soil failure during seismic activity. The shear wave velocity ( $V_s$ ) chart has been utilized extensively in recent decades because of its non-invasive nature and adaptability to a broad variety of soil types. This graphic was created using data from both field and lab studies. Research indicates that the capacity to liquefy short- and dense-density sands grows more quickly compared to the case of loose sands as relative density rises. This suggests that the pattern of destabilization resistance development may depend on the kind of failure. Flow liquefaction and cyclic mobility must be included for sands with varying densities to improve the accuracy of  $V_s$ -based models (Nejad, Momeni, & Manahiloh, 2018).

## **2.6 Maximum Shear Modulus ( $G_{max}$ )**

While many studies have focused on predicting the maximum shear modulus ( $G_{max}$ ). Generally,  $G_{max}$  values decrease as FC increases. This trend has been observed where parameter A in the predictive equation is influenced by FC and void ratio ( $e$ ), while parameter n remains relatively constant and unaffected by FC. This reduction in  $G_{max}$  with increasing FC has been confirmed by several studies. However, some research has shown that for a constant relative density ( $D_r$ ),  $G_{max}$  increases with FC up to 20% and decreases when FC exceeds 20%. Additionally, the rate of increase in  $G_{max}$  slows as FC continues to rise (Muduli & Das, 2015). This finding differs from other research indicating that for a constant void ratio,  $G_{max}$  decreases with increasing FC below

10% and then stays nearly constant beyond that point (Shahri, Behzadafshar, & Rajablou, 2013). Experimental data suggest that the transition from sand-dominated to fines-dominated behavior in sand-fines mixtures occurs gradually when FC ranges from 10% to 25%. Furthermore, significant variations in the parameter  $n$  of the predictive equation were observed with increasing FC, although some studies noted that  $n$  remains generally insensitive to changes in FC. These varying observations underscore the complexity of predicting  $G_{\max}$  in sandy soils with different fines contents and suggest a need for more comprehensive studies to fully understand these relationships (Shahri et al., 2013).

## **2.7 Shear Stress ( $\tau$ )**

Understanding how soil behaves under seismic loading requires an understanding of shear stresses and soil dynamics. Soil liquefaction can occur because of the dynamic reaction of soil to shear pressure during an earthquake, which presents serious concerns to the integrity of infrastructure and buildings. The link between shear stress, soil factors, and liquefaction is examined in this overview, which also highlights significant discoveries and advancements in the subject. The internal resistance that soil particles show to external pressures, such as those produced during an earthquake, is known as shear stress in soils (Huang, Chen, & Zhao, 2015). The general strength and deformation properties of the soil are significantly influenced by the amount and spatial distribution of shear stress present in its layers. Predicting the behavior of soils in response to seismic occurrences requires an understanding of the changing characteristics of soils under conditions of cyclic loading. Numerous studies have demonstrated that the shear strength and deformation resistance of soil are highly influenced by several soil parameters, such as moisture content, density, and grain size distribution (Ji, Kim, & Kim, 2021). Via repeated application and absorption of shear stress brought on by the cyclic loading imposed by seismic waves, variations in pore water pressure and successful stress within the soil matrix result. These modifications have a crucial role in predicting whether the soil would liquefy. Advancements in soil dynamics have led to the development of various analytical and numerical models that simulate the behavior of soils under seismic loading. These models incorporate factors such as strain rate dependency, hysteresis, and damping characteristics of soils, providing a more comprehensive understanding of soil response under dynamic conditions. Laboratory tests, such as cyclic triaxial and direct simple shear tests, have been instrumental in characterizing the dynamic properties of soils and

validating these models. Soil liquefaction is a transient transition from a solid to a liquid form caused by an increase in pressure in the pores that causes saturated, loose, sandy soils to lose their strength and rigidity. The primary cause of this phenomena is the cyclic shear forces produced by an earthquake. Understanding the beginning, spreading, and impacts of this process on the soil's resilience and structural integrity is all included in the research of soil liquefaction. The goal of early studies on soil liquefaction was to determine the circumstances that are most likely to lead to liquefaction. Based on observation in the field and laboratory testing, empirical correlations were created linking the probability of liquefaction to variables such soil type, the relative density, and seismic intensity. The liquefaction assessment techniques that were initially developed and extensively applied in engineering practice were based on these relationships. More complex methods, including dynamic principles and sophisticated soil mechanics, were included in later research to increase the precision of liquefaction forecasts. With the creation of the cyclic resistant ratio (CRR) and its comparison with the cyclic stress proportion (CSR), soil behavior under cyclic loading has been better understood. This method allowed engineers to balance the stresses being applied and soil resistance, allowing them to more accurately assess the likelihood of liquefaction. The influence of soil characteristics' spatial variability on liquefaction potential has been investigated in more detail. To evaluate the variability of soil deposits and improve evaluations of the liquefaction danger, techniques including geostatistical approaches and in situ testing (e.g., cone testing for penetration, shear wave velocity studies) have been used. These developments have made it easier to create comprehensive maps of the liquefaction hazard, which are essential for risk reduction and urban planning (Kokusho, 2013). Ground deformation caused by liquefaction can take many different forms, such as lateral spreading, ground fissures, and settlement. These deformations can cause severe damage to buildings, lifelines, and other infrastructure. Understanding the mechanisms behind these deformations and developing strategies to mitigate their impacts have been key areas of research. Ground improvement techniques, such as soil densification, drainage, and reinforcement, have been studied and implemented to reduce the susceptibility of soils to liquefaction. The interplay between shear stress, soil dynamics, and liquefaction is a complex and critical area of study in geotechnical engineering. Advances in understanding the dynamic behavior of soils and the mechanisms of liquefaction have significantly improved the ability to predict and mitigate the risks associated with seismic events. Ongoing research continues to enhance these predictive models and

mitigation techniques, contributing to the resilience of structures and infrastructure in earthquake-prone regions.

## **2.8 Liquefaction Potential Index (LPI)**

(M.Y. Khan et al 2021) utilized the technology of electrical resistivity tomography by having three zone of layers under the ground such as discontinuous zone of medium resistivity, high zone made up of basal layer overlaid by the low zone. The certain founding was that ground water was increased due to earthquake of 2019, Mirpur and also found sand blows, ground fractures in to the zone of maximum shaking. A new technique was again applied by using ground penetrating radar (GPR) and PSINSAR by finding the coseismic liquefaction hazard in the upper most 5 m layers of soil along with high ground water table which raised excess pore water pressure (Younis et al. 2023). The Liquefaction Potential Index (LPI) has been developed as a quantitative measure to evaluate the likelihood and severity of soil liquefaction over a specific area (Hossain, Roknuzzaman, & Rahman, 2022). To give a thorough evaluation of the risk of liquefaction, LPI incorporates several variables, such as seismic characteristics, groundwater conditions, and soil qualities. To reduce damage during seismic occurrences, this index helps planners and engineers identify locations that are susceptible to earthquakes and put suitable mitigation measures in place.. The primary empirical correlations used in the assessment of liquefaction potential in the past were from field observations and case studies. These techniques concentrated on specific soil layers and their liquefaction susceptibility, but they frequently overlooked the combined impacts of many layers and the general site circumstances (GASHAW, 2020). The LPI was created by researchers as a more comprehensive technique once they became aware of these limitations. To determine the likelihood of surface manifestation of liquefaction, the LPI considers the depth, thickness, and characteristics of soil layers in addition to the magnitude of ground shaking. It is a helpful tool for risk assessment and urban planning since it gives a single number that represents the degree of possible liquefaction-induced ground deformation. Numerous studies have confirmed that LPI is successful in many seismic zones and that it can be used to a range of soil types and earthquake scales. By adding complex modeling tools and cutting-edge geotechnical data, researchers have further improved the LPI. These improvements have increased the LPI's usefulness in both practical and research applications and increased the precision of liquefaction forecasts. Furthermore, the spatial depiction of liquefaction risk made possible by the integration of LPI

using Geographic Information Systems, or GIS, has improved decision-making for infrastructure construction and land use planning. Planners and engineers can identify high-risk sites and prioritize mitigation actions by mapping LPI values throughout a region (Kayabasi & Gokceoglu, 2018). The LPI is not without difficulties, despite its achievements. The quality and precision of input data, which can fluctuate greatly between sites, determines how accurate LPI forecasts are. Furthermore, uncertainties arising from the dynamic character of seismic occurrences and soil behavior need to be properly handled. These issues are still being researched, with the goal of improving the LPI's resilience and reliability as a forecasting tool. An important development in the realm of geotechnical engineering is the Liquefaction Probability Index (LPI), which offers a thorough and useful method for evaluating liquefaction risk. Its creation and improvement have been motivated by the need for trustworthy and useful information to safeguard infrastructure and populations against the catastrophic impacts of earthquakes (Kim, Kim, Baise, & Kim, 2021).

## **2.9 Overview of Machine Learning**

Machine Learning, a branch of artificial intelligence, emphasizes the creation of algorithms and models that enable computers to undertake tasks autonomously, without the need for specific programming for each task. Essentially, a machine learns from data to find patterns and make predictions or decisions without any human interference. These machine learning algorithms have shown immense potential in solving complex problems across various domains (Pulina, 2010). The application of diverse machine learning algorithm portfolios is suggested for tackling intricate tasks in robotics and automated reasoning. Unlike traditional algorithms that follow a strict set of instructions, ML algorithms adapt and learn from the data they're provided. This means they can discover hidden patterns or subtle relationships in vast amounts of data that might be challenging or time-consuming for humans to discern (Erzin & Tuskan, 2019). Once trained, many ML models can adapt over time by learning from new data, allowing them to stay relevant in changing environments ". ML algorithms are designed to take a broad view from the training data to unseen scenarios, which means they can handle a variety of situations do not present in the initial training set. Deep learning models, which fall under the umbrella of ML, have the capability to autonomously extract features from unprocessed data, eliminating the need for manual feature engineering. This attribute renders them highly effective in tasks such as image and speech recognition. ML models, especially specific types like RF or Neural Networks (NN), can handle



high-dimensional data effectively, capturing interactions between various features. For tasks like data clustering or image recognition, manually defining rules or patterns would be cumbersome. ML models can automatically and efficiently handle these tasks after being trained on representative data.

### 2.9.1 K-Nearest Neighbors (KNN)

One of the most straightforward machine learning methods based on the technique of supervised learning is the algorithm for k-nearest-neighbors, often known as k-NN or KNN. It places the new sample in the group to which it is most comparable, assuming that the new and present data are similar. It is possible to apply the KNN approach to classification as well as regression. The KNN method works as follows: an exact approximation of K is selected, and since K must be an odd integer, the more precise the result. To maximize outcomes, different k-values and distance measurement metrics (consistent and distance) have been included in the Research settings. This allowed for a methodical exploration of various parameter combinations and the ten-fold cross-validation process to identify the optimal effect parameters. In this investigation, setting the neighbors to 4 and the Weights to "distance" produced the KNN algorithm's most accurate results.

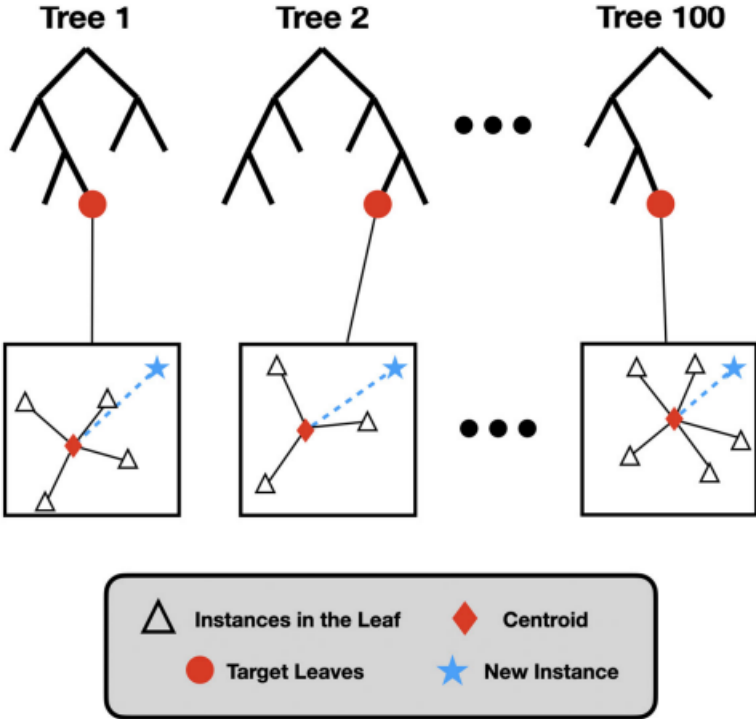


Figure 2.1: K-Nearest Neighbors prediction model architecture

## 2.9.2 Random Forest Algorithm

It is a versatile and widely used algorithm which belongs to the ensemble learning category. It uses a collection of decision trees to perform regression and classification tasks (Liu et al., 2012) and a graphical visualization of RF model is shown in Figure below. RF has been applied to many domains, including image classification, generating continuous field datasets, detection of spam mails, detection of credit card fraud, classification of genes, detection of network intrusion, email spam detection, gene classification, credit card fraud detection, and text classification (Horning, 2010; Zakariah, 2014).

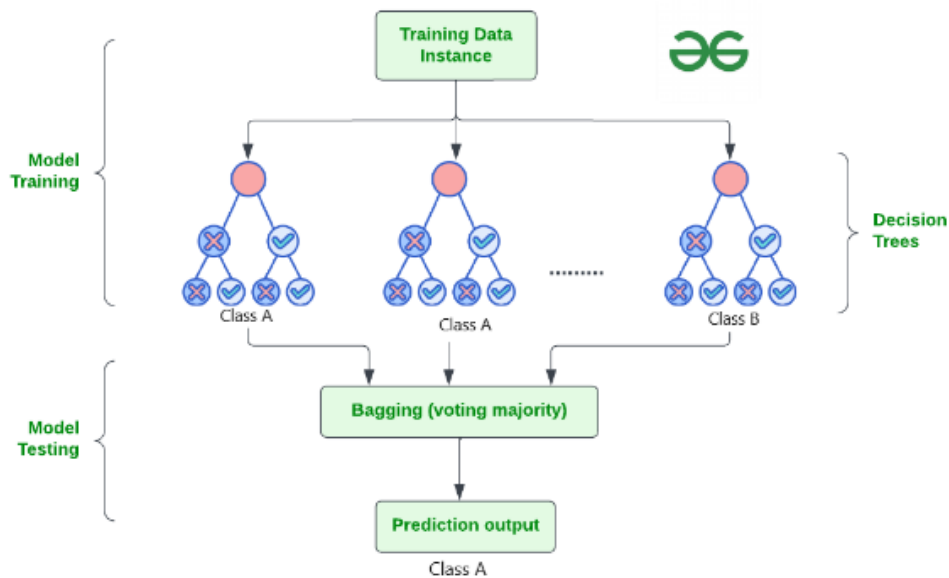


Figure 2.2: Random Forest prediction model architecture

## 2.9.3 Support Vector Regression (SVR)

It's a type of Support Vector Machine which is used for regression tasks. And SVM is mainly known for classification, SVR is its adaptation for predicting continuous values. SVR, or Support Vector Regression, learns directly from the data how important different variables are in explaining the connection between inputs and outputs. This is a step away from older regression methods, which often rely on assumptions that might not match the real-world data perfectly. SVR stands out because it figures out the value of variables directly through the data it analyzes, offering a more tailored approach to understanding data relationships and is shown in Figure 6. SVR has

been applied successfully to analyze brain imaging data and reveal patterns through multiple brain regions for various disorders(Amroune, 2022).

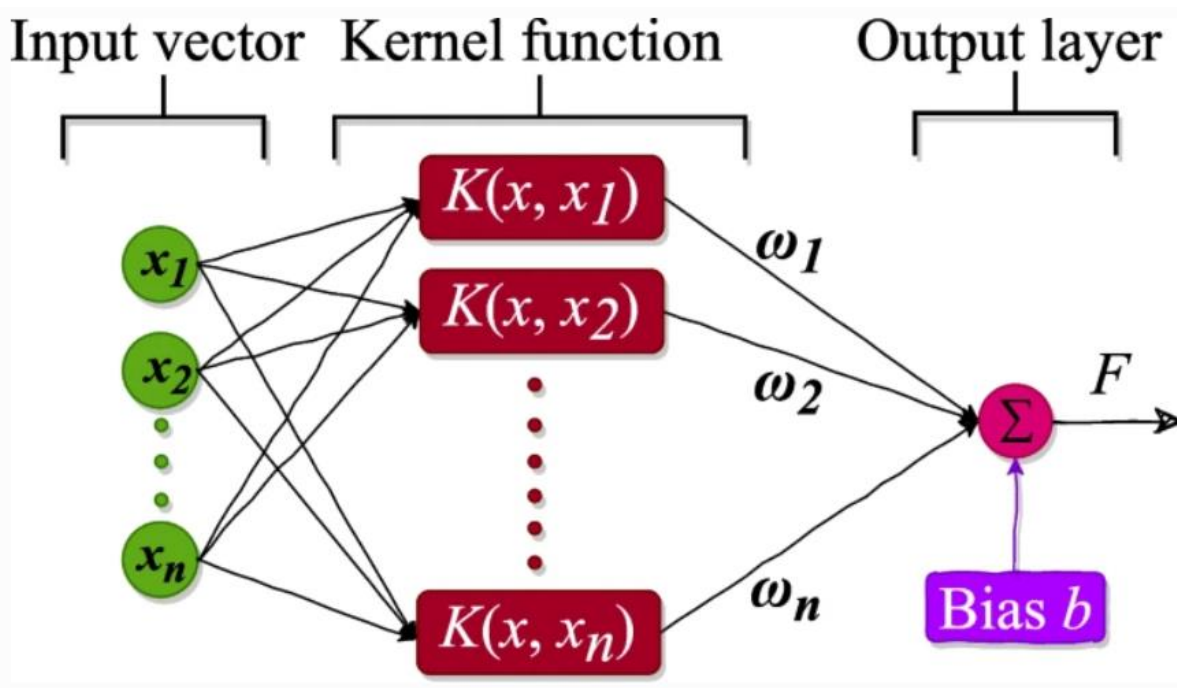


Figure 2.3: Support vector machine model architecture

#### 2.9.4 XGBoost Algorithm

XGBoost, short for Extreme Gradient Boosting, is a powerful tool that takes gradient boosting to the next level. It's crafted to work quickly and adaptively, making it a go-to for tackling big data challenges. Essentially, it's like having a supercharged engine for your data analysis, capable of handling tasks with speed and agility that traditional methods can't match (Chen & Guestrin, 2016). It works for both regression and classification problems (Tran et al., 2024). A flow chart diagram of XGBoost is shown in Figure below.

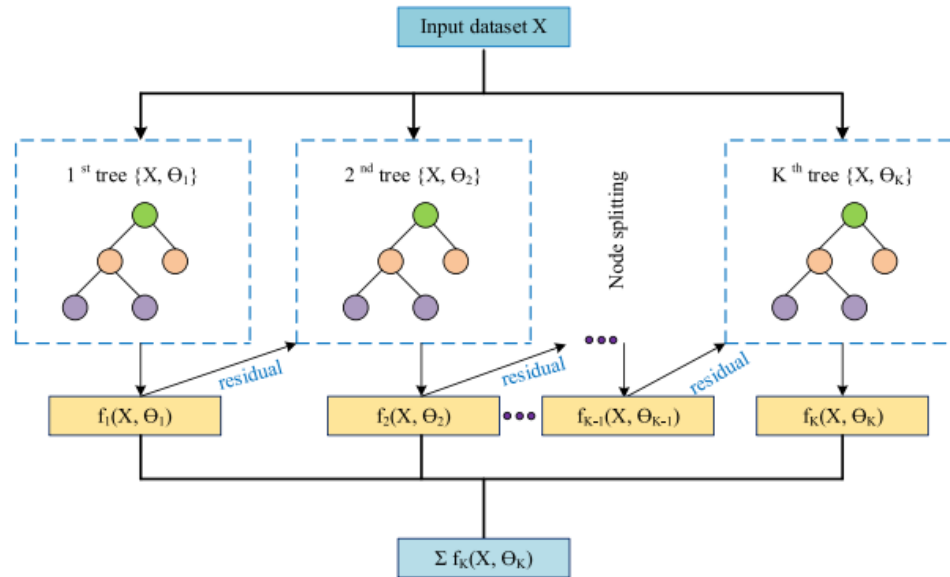


Figure 2.4: Extreme Gradient Boost prediction model architecture

### 2.9.5 Decision Tree

Decision trees (DT) are a well-liked technique for regression or classification that yields accurate and simple-to-understand results' algorithms come in several varieties, but they all share a common framework. The algorithm, to put it succinctly, divides the data set into consecutive subsets in accordance with predetermined criteria. Tree-like structures can be used to graphically depict this process. Non-parametric DTs exist. They can simulate intricate interactions and do not make any assumptions about how the variables are connected (Ghani & Kumari, 2022).

- They deal with data that is heterogeneous (comprising of both categories and numbers).
- Because DTs choose the most crucial variables to use in their own operations, they are somewhat resistant to unimportant variables.
- They withstand sorting mistakes and outliers equally well.
- Even for those who have no prior experience with statistics, they are simple to understand.
- Division rules, stop criteria, and assignment rules are the three components that go into creating a decision tree.

A query whose response splits the set at the node's level into multiple subsets or more is referred to as a division at that node. Depending on the kind of decision tree selected, these queries or division rules change. Following the application of these criteria to every variable

in the collection, the variables are ranked in accordance with the data they yield, identifying the most valuable division as a node.

### 2.9.6 Gradient Boost

Based on the error function, the gradient boosting technique is an optimization technique. Machine learning techniques like gradient boosting are used to address regression and classification issues. By combining weak prediction models, like the decision tree, it creates a powerful prediction model. After that, Friedman built the GBRT algorithm. The fundamental notion is that a basic model performs each calculation, and the subsequent calculation is carried out to lower the residual of the previous model and build a new basic model that points in the gradient's direction with lower residuals (Das & Muduli, 2011). Thus, the loss function may be decreased and optimized by continuously modifying and improving the weight. The following algorithm parameters were chosen for this study: loss = "least squares," learning\_rate = 0.1, subsample = 1.0, n\_estimators = 100, max\_depth = 3, alpha = 0.9, min\_samples\_N = 1, and max\_N = 0. The loss function for a collection of data points  $(x_i, y_i)$ , where  $i=1, \dots, N$ , may be written as  $gm(x)$ . There are discontinuous zones created in the input space.  $1m$

For every area  $bjm$ ,  $R2m$ , ...,  $Rjm$ , and a constant value is estimated. Regression trees have  $j$  leaf nodes in total.

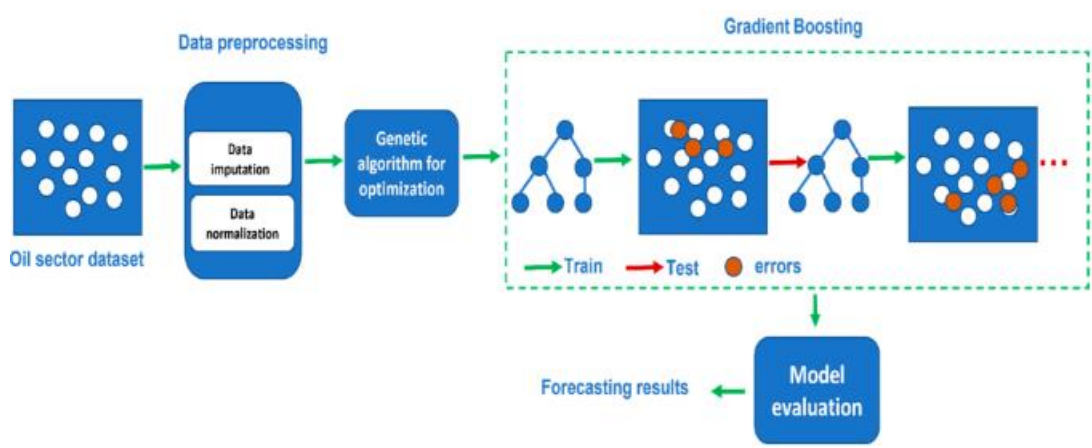


Figure 2.5: Gradient Boost prediction model architecture

### 2.9.7 Artificial Neural Network

The Sicilian soil database's generalized feedback (GFF) neural network was shown to be the most effective model for simulating soil water retention. A popular model for simulating physical

processes, the multi-layer perceptron (MLP) is generalized in this artificial neural network (ANN). Any neuron in a hidden layer of an MLP gets input from every other neuron in the layer before it and delivers its output to every other neuron in the layer after it. GFF contains connections between neurons in layers that are not contiguous, unlike MLP (Fahim, Rahman, Hossain, & Kamal, 2022). The term "feed-forward" refers to these kinds of networks since the signals only move from the point of entry to the output. Moreover, supervised learning is typically used to train them, which entails using a subset of observed input and output pairings. One input layer, two layers that were concealed with fifteen neurons apiece, and one layer of outputs made up the ANN design suggested in this work. Depending on the set of parameters being entered used, the input layer's neuron count ranged from three to four. Using a backpropagation technique with a momentum term, which adjusts weights along an error gradient to increase network convergence, the ANN training phase was carried out. 0.1, 0.001, and 0.1 learning rates were used for the input layer, first hidden layer, and second hidden layer connections, respectively. For every layer, the speed factor was 0.6. Online updates were made to the weights following the display of each input pattern (Kayabasi & Gokceoglu, 2018).

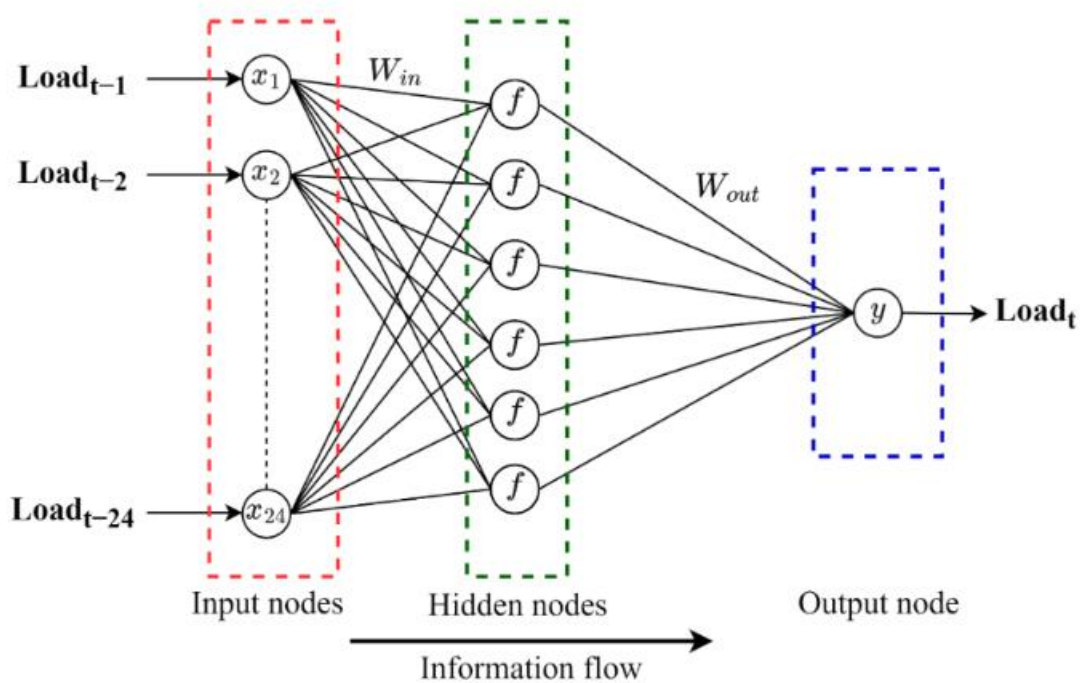


Figure 2.6: ANN prediction model architecture

## 2.10 Model Evaluation Metrics

Model evaluation is like a check-up for your machine learning model, ensuring it's smart enough to handle new, unseen data. It's about tweaking its learning settings and making sure it's not just memorizing but truly understanding, ready to face real-world challenge.

There are two types of model metrics. One is for regression and the second is for classification. The regression metrics are given below.

$$RMSE = \sqrt{\left(\frac{1}{n}\right) \times \sum_{i=1}^n [p_i - y_i]^2} \quad (2.11)$$

$$MAE = \frac{1}{n} \times \sum_{i=1}^n (|p_i - y_i|) \quad (2.12)$$

$$R^2 = 1 - \frac{\sum_{i=1}^n (y_i - p_i)^2}{\sum_{i=1}^n (y_i - \bar{y})^2} \quad (2.13)$$

Where:

$n$  = sample size

$p_i$  = predicted values

$y_i$  = actual values

$\bar{y}$  = average of actual values

These metrics are typically specific to the context of a study and depend on the data's nature, the model's complexity, and the field of application. Generally, for  $R^2$ , a value closer to 1 indicates a better fit, while for RMSE, a lower value indicates a better fit. However, standard reference values may not be universal and can vary based on the domain or specific application.

## Chapter 3: Methodology

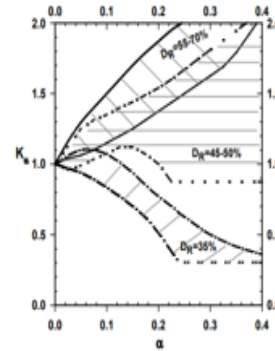
The methodology for utilizing the machine learning algorithms to evaluate the dynamic properties and liquefaction properties of soil involves the several key steps. The methodology includes the study area for the exploration of soil data, soil profile and parameters for data collection, estimation of liquefaction potential index (LPI) using standardized correlation (Abdullah Ansari, Falak Zahoor, 2022), data pre-processing and screening for used as input dataset for machine learning models, and the experimental setup which includes the model's architecture. The flowchart for the estimation of liquefaction potential index (LPI) and detailed methodology is shown in figure 1 (a) and (b) below.

LPI Estimation

$FS = \frac{CRR}{CSR}$	$CRR_{M,\sigma'_v} = CRR_{M=7.5,\sigma'_v=1 \text{ atm}} \cdot MSF \cdot K_\sigma \cdot K_\alpha$
	$CSR = 0.65 \cdot \frac{\sigma_v}{\sigma'_v} \cdot \frac{a_{max}}{g} \cdot r_d$ $MSF = 6.9 \cdot \exp\left(\frac{-M}{4} - 0.058\right) \leq 1.8$
$CRR_{M=7.5,\sigma'_v=1 \text{ atm}} = \exp\left\{ \frac{(N_1)_{60cs}}{14.1} + \left[\frac{(N_1)_{60cs}}{126}\right]^2 - \left[\frac{(N_1)_{60cs}}{23.6}\right]^3 + \left[\frac{(N_1)_{60cs}}{25.4}\right]^4 - 2.8 \right\}$	
$F(z) = 1 - F_x$ , for $F_x < 1.0$ $F(z) = 0$ , for $F_x \geq 1.0$ $W(z) = 10 - 0.5z$ , for $z < 20 \text{ m}$ . $W(z) = 0$ , for $z > 20 \text{ m}$	$r_d = 1.0 - 0.00765 \cdot z$ $z \leq 9.15 \text{ m}$ $r_d = 1.174 - 0.0267 \cdot z$ $9.15 \text{ m} < z \leq 23 \text{ m}$

The LPI can be determined as follows:

$$LPI = \int_0^{20} F(z) \cdot W(z) dz$$



$$K_\sigma = 1 - C_\sigma \ln\left(\frac{\sigma'_v}{P_s}\right) \leq 1.1$$

$$C_\sigma = \frac{1}{37.3 - 8.27(q_{c150})^{0.234}} \leq 0.3$$

$$C_\sigma = \frac{1}{18.9 - 2.55\sqrt{(N_1)_{60cs}}} \leq 0.3$$

Figure 8. Relationship between  $\alpha$  and  $K_\sigma$  (after Harder and Boulanger, 1997)

Whereas,

FS = Factor of Safety

$a_{max}$  = Peak ground surface acceleration

$CRR_{M=7.5,\sigma'_v=1 \text{ atm}}$  = Cyclic Resistance Ratio at earthquake magnitude of 7.5

MSF = Magnitude Scaling Factor

$\sigma_v, \sigma'_v$  = Total and effective vertical Stress.

CSR = Cyclic Stress Ratio

$(N_1)_{60cs}$  = SPT-N count (N) equivalent clean sand (CS) corrected

Rd = Reduction Factor calculated in terms of depth, z in meters



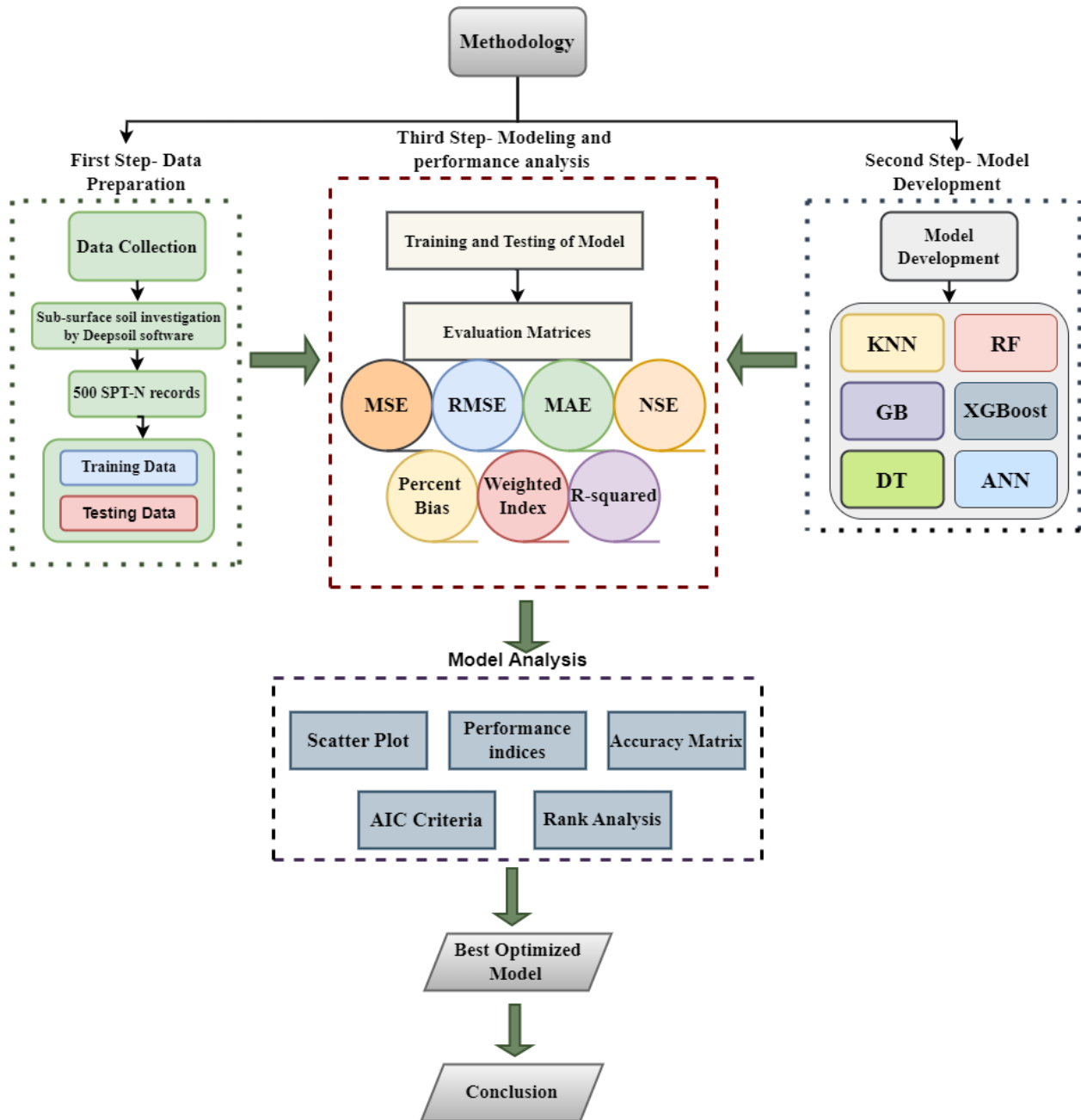


Figure 3.1: Methodology flow charts

### 3.1 Study area

Subsurface soil research has been conducted for the locations around Bhimbar and Mirpur shown in Figure 2 in order to assess soil liquefaction potential using SPT-N values. This has been followed by nonlinear seismic site response analysis (NL GRA) of the explored soil data. The locations selected for liquefaction potential and dynamic property assessment are close to the Jhelum River

bridge centers. To demonstrate the application of the soil investigation data, nonlinear ground response analysis (NL GRA) has been performed along Jhelum River in Mirpur, a northeastern of Pakistan, classified as one of the active regions of the country surrounded by many tectonic faults. The nonlinear ground response analysis was performed on three implemented soil columns. The profile is explored near the center of the bridge and flyover in Jhelum River. The explored depth consists of sand with increasing relative density; therefore, the chosen soil profile is assumed to be underlain by a bed rock beyond the exploration data. Because the chosen profile is close to a river, the soil columns are primarily made up of sand with a range of shear wave velocities in (Figure ). According to the Economic Affairs Division, Pakistan, earthquake 2005 & 2019 has caused several death approxing 80000 people, injuries reached to 70000. No of houses destroyed by the earthquake was 203,579 while damaged 196,576 houses. (S.M. Ali et al. 2011) there were more than 90 bridges damaged by the earthquake. The 2019 Bhimbar and Mirpur earthquakes, which caused liquefaction failure, inspired researchers to assess the dynamic reaction of soil. Therefore, whether conducting seismic requalification of existing structures or seismic resistant design of new buildings, evaluation of the dynamic characteristics and liquefaction potential of soil in one of the active seismic zones is highly beneficial.

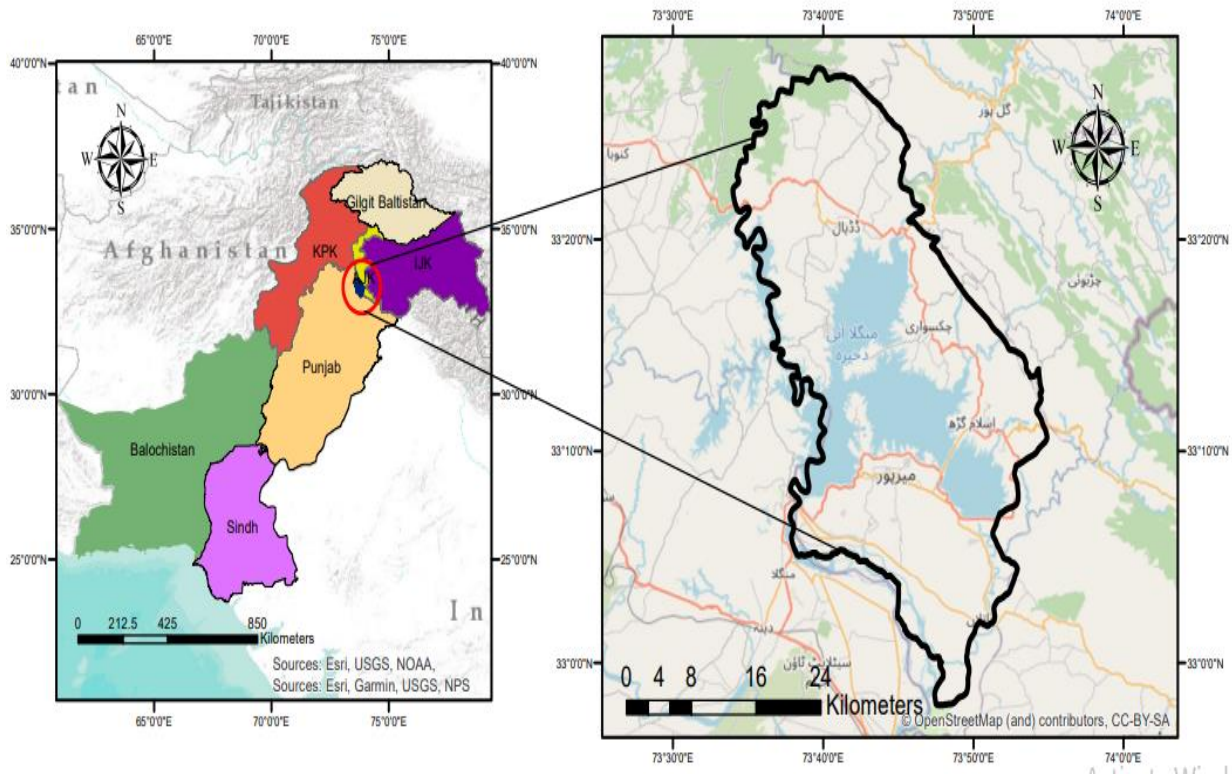


Figure 3.2: Study area map

### 3.2 Soil Profile

Subsurface soil research has been conducted for the locations around Jhelum and Mirpur shown in Figure 1 to assess soil potential for liquefaction using SPT-N values. This has been followed by nonlinear seismic site reaction analysis (NL GRA) of the explored soil data. Since the profile that was chosen is close to a river, the sites were chosen for a dynamic evaluation. As a result, the soil columns primarily consist of sand with changing shear wave velocity. 2019 saw a liquefaction failure brought on by an earthquake. The Mirpur earthquake motivated the researchers to evaluate the dynamic response of soil. Therefore, to execute seismic requalification of current structures or seismic resistance design of new buildings, evaluation of the dynamic characteristics and liquefaction potential of soils in one of the active seismic regions would be beneficial. Properties and potential for liquefaction are located close to the middle of the Chenab River and Jhelum River bridges for Sites 1-4, which have water table depths of 1, 1.5, 2, and 3 meters, respectively.

### 3.3 Data Collection

Since nonlinear seismic site reaction analysis uses a more realistic method than the corresponding linear technique, it is undertaken in comparison with the latter. To assess the elevated pore water pressure ratio for the earth's columns under consideration, this study took the same into account. The study was carried out using version 7.0 of the DEEPSOIL program. The software that is now available proposes standard curves for evaluating dynamic features. The thickness of each of the layers is modified for every exploration data so that a layer can propagate at a maximum frequency greater than 30 Hz. The bed rock is represented as an elastic half area with a shear wave velocity of 760 m/s, a density of 25 kN/m<sup>3</sup>, and a damping value of 2%. The necessary input variable for the study is assessed based on SPT-N values in line with the following equation of (Ohsaki and Iwasaki, 1973) in ton/m<sup>2</sup> for cohesionless soils since there was no calculated maximum shear modulus (G<sub>max</sub>) data available.

$$G_{\max} = 6.50N^{0.94} \quad (1)$$

The unaffected soil investigation data was utilized to import the analysis's input parameters, and the DEEPSOIL hyperbolic and pressure-dependent MRDF-UIUC process was employed to fit the given data points. A suggested soil model was employed to assess the enhanced PWP production and dissipating of soil columns taken into consideration in this investigation. The information was gathered through experimental testing and fieldwork. Over five hundred soil property records were gathered. A broad range of soil kinds, characteristics, and specific soil weights are covered in the database.

Two principles, were followed for pile bearing capacity determination: either the settlement of pile top at the current load level was at least 5 times that of settlement at the previous load level, or a linear load-settlement curve was observed. The bearing capacity was defined as the load level at which the settlement exceeded 10% of the pile diameter. This comprehensive dataset of static load tests on pre-cast reinforced concrete piles is substantial and forms a robust foundation for developing and validating advanced machine learning models, which is a key aspect of this research. The introduction of parameters is given in Table 3.1 and statistical summary of input is given in Table 1.

Table 3.1: Introduction of input parameters

Parameters	Count
SPT-N	500
Shear Stress (ton/m <sup>2</sup> )	500
Gmax (ton/m <sup>2</sup> )	500
Vs (m/s)	500
PGA <sub>surface</sub> (g)	500
rd (meter)	500
MSF	500

### 3.4 Data screening

Large datasets can be affected by outliers, and improving efficiency often involves their removal, even though it may reduce errors in the analysis. Outliers can be identified using a box plot based on variance and median. However, caution should be exercised, and observations should not be discarded unless there is certainty that the outlier is due to measurement error or has a significant impact on the model.

- The authors of the research work have chosen to use 80% of the total data as their training dataset. That is, 80% of 500, which equals 400 SPT-N case histories.

The remaining 20% of the data, which amounts to 100 SPT-N case histories (20% of 500), is designated as the testing dataset. The purpose of this testing dataset is to assess and evaluate the performance of the models after they have been trained on the training dataset.

### 3.5 Removing Outlier:

Datasets become massive due to outliers, which should be removed to improve efficiency even though it narrows down the error to correct the result. Soil dynamics properties monitoring data

may have some outliers. Abnormal values can be obtained during monitoring. These values may affect the quality of the monitored data. Before building any model, observed data must be checked outliers by the Grubb test. The Grubbs test was developed to determine whether the greatest value or the lowest values are outliers. In this study, outliers can be removed from the data set and the nonlinear partial least squares algorithm (NIPALS). Research data were standardized before proceeding to build training models. In this study, data were normalized in the 0–1 range using the linear scale method.

$$X_{normalized} = \frac{(x - x_{min})}{(x_{max} - x_{min})} \quad (2)$$

Where x is the observed value, and x min and x max are the minimum and maximum value in the data set.

With careful consideration to statistical details, the data division procedure was carried out to create training and testing datasets, guaranteeing that important parameters like minimum, maximum, mean, and standard deviation were evenly distributed throughout the datasets. This meticulous statistical consistency was essential to maximizing our models' performance and, as a result, supporting a comprehensive assessment of them. The statistical properties of the input variables, such as the mean, standard deviation, minimum, and maximum for the training and testing datasets, are shown in Table 2.

Table 3.2: Statistical dataset

<b>Variables</b>	<b>SPT-N</b>	<b>Gmax (ton/m<sup>2</sup>)</b>	<b>Vs (m/s)</b>	<b>Shear Stress (ton/m<sup>2</sup>)</b>	<b>Peak Ground Surface Acceleration (g)</b>	<b>Reduction Factor rd (m)</b>	<b>LPI</b>
<b>Minimum</b>	3	17.902	98.76	0.000	0.583	0.51	0.007
<b>Maximum</b>	30	131.364	621.50	8.304	1.173	0.943	3.935
<b>Mean</b>	9	70.641	438.721	0.737	0.8361	0.641	1.8
<b>Standard Deviation</b>	6.271	36.819	147.597	1.216	0.133	0.0739	1.637
<b>Variance</b>	39.321	1355.648	21784.889	1.480	0.0177	0.006	2.679
<b>Range</b>	22	113.462	522.741	4.601	0.367	0.492	3.928

We evaluated the models we constructed in terms of their predictive power and generalization performance by dividing the sample suitably. The models showed impressive similarities in their performance on the training and testing datasets, indicating that our models are not overfitting but rather are able to apply their learned information to the trained ranges. Our models are well-suited to handle real-world scenarios with precision and reliability because of their resilience and uniformity in performance, which gives us confidence that they may be used successfully in practical applications within the designated data ranges.

### **3.6 Data Partition:**

Once the dataset is meticulously preprocessed, the next step is its splitting into distinct sets for model training and validation. The partitioning was carried out using the ``training, testing and validation`` function from the Scikit-learn library. This function not only ensures a random distribution of data points into the two sets but also guarantees consistency in this random division. The result is a balanced and representative split that highlights effective model training and validation. For the current dataset, the data is split with a ratio of 90:10 and reasons are:

- 90% of the data is allocated towards the comprehensive process encompassing hyperparameter optimization, training, and internal validation of the model settings. This data is labeled as “training and testing data” and it will ensure that the model has enough information to understand and capture relationships and patterns.
- The remaining 10% is reserved for validation purposes of proposed tuned models and labeled as “validation data”.

### **3.7 Experimental Setup**

Using an Intel 2.20 GHz CPU for testing and a Windows 10 PC with a GeForce 980 GTX GPU, Python is employed to train the models. Google partnered with NVIDIA to supply GPUs and CPUs to speed up calculations. The investigation was conducted using Python 3.8, and Google Colab provided 16 gigabytes of RAM for the experimentation. Additionally, Google Colab is a helpful tool for running code and conducting tests because of its user-friendly interface and compatibility with Python. To accommodate larger datasets and memory-intensive operations, the platform additionally offers a substantial 16 gigabytes of RAM for the studies. It is an open-source machine learning library for Python that offers simple and efficient tools for data analysis and modeling. It

provides a range of supervised and unsupervised learning algorithms, is built upon the SciPy (Scientific Python) library and is known for its ease-of-use and versatility. RF Regressor, SVR, and XGBoost are carefully imported into python.

### 3.8 Architecture of Models

This section outlines the supervised classification that is employed in this study. This study uses several machine learning (ML) and Deep learning (DL) models, which are discussed in this section.

#### 3.8.1 K-Nearest Neighbors (KNN)

One such approach is K-Nearest Neighbors (KNN), which continues to perform rather well for huge training sets despite its simplicity (Maillo J. et al. 2017). It only depends on the most fundamental premise of any prediction, which is that comparable observations will typically provide similar results. The vast majority (often weighted) of a new observation's k "Nearest Neighbors" in the training set is used by Nearest Neighbor techniques to forecast a new observation's value (Richman et al. 2011). If an observation is given an infinite quantity of data, it will have many "neighbors" that are arbitrarily close to each other in terms of all characteristics measured, and the variability of their results will yield as accurate a prediction as is possible in theory, unless there is a completely specified model (Pandey et al. 2017). But since we can never have enough data, this asymptotic property's real usefulness is debatable, particularly for small datasets.

```
[ ] # Create a KNeighborsRegressor model
    k_neighbors_model = KNeighborsRegressor(n_neighbors=4)
    # Evaluate the classifier using the function
    r2_score_result1 = evaluate_regression_model(k_neighbors_model, X_normalized_train, y_normalized_train,

    print(f"R-Square: {r2_score_result1}")
```

R-Square 0.9903815811179542

Figure 3.3:K-Neighbors prediction model code



### 3.8.2 Random Forest (RF)

One popular machine learning approach for regression tasks is called RF. Several decision trees are used in this ensemble approach to decrease over fitting and increase prediction accuracy. RF is superior to conventional machine learning algorithms in several ways, including its handling of missing values, high-dimensional data, and nonlinear correlations between variables (Rigatti et al. 2017). Furthermore, it offers changeable relevance measurements that may be applied to feature interpretation and selection. One of the most widely used Python applications for RF classification and regression. It provides a simple interface for building and evaluating RF models and handles both regression and classification operations.

```
# Create a Random Forest Regressor
rfreg = RandomForestRegressor(n_estimators=100, random_state=42)

# Evaluate the model and store the R2 score
Matric_rf = evaluate_regression_model(rfreg, X_normalized_train, y_normalized_train, X

# Print the R2 score
print(f"R-Squared: {Matric_rf}")

<ipython-input-25-88953cdcaf16>:3: DataConversionWarning: A column-vector y was passed
  regressor.fit(X_normalized_train, y_normalized_train)
R-Square 0.9905819464632069
```

Figure 3.4: Random Forest prediction model code

### 3.8.3 Gradient Boosting (GB)

Like random forests, Gradient boost is a machine learning technique for regression problems that creates predictions by aggregating the results of many decision trees. Gradient trees employ decision trees to detect learners who are not proficient (Si. S. et al. 2017). With the idea of residuals, gradient boosting calculates the difference between the current prediction and the actual target value. Following the residual's determination, the approach transfers the weak attributes to it, continuously pushing the model closer to the target value. By repairing the errors of the previous three trees, gradient boost regression constructs one tree at a time as opposed to random forest. Though the computational cost is higher, the final output is more accurate (Lusa et al. 2017).

```

gb_model = GradientBoostingRegressor(n_estimators=100, learning_rate=0.05, random_state=42)
Matric_gb = evaluate_regression_model(gb_model, X_normalized_train, y_normalized_train, X_normalized_test, y_normalized_test)

# Print the R2 score
print(f"R-Square: {Matric_gb}")

```

```

/usr/local/lib/python3.10/dist-packages/sklearn/ensemble/_gb.py:437: DataConversionWarning: A column-vector y was passed when a 1d
y = column_or_1d(y, warn=True)
R-Square 0.9922608682495786

```

Figure 3.5: Gradient Boost prediction model code

### 3.9 Extreme Gradient Boosting (XGBoost)

Extreme Gradient Boosting is a technique that has gained popularity recently because of its exceptional accuracy and efficiency. A group method known as XGBoost combines multiple ineffective learners, like decision trees, into a single, strong learner. The approach adds decision trees to the model iteratively, with each tree seeking to correct the flaws of the previous one. The XGBoost package is frequently used in R to execute the XGBoost regression model (Chen et al. 2016). The XGBoost package also offers support for hyperparameter tweaking, which could significantly improve the model's performance. The hyper parameters, which include learning rate (eta), number of trees, maximum depth of each tree (max, depth), and regularization factors (gamma and alpha), can be fine-tuned in multiple ways.

```

] xgb_model = xgb.XGBRegressor(n_estimators=100, learning_rate=0.05, random_state=42)
# Evaluate the model and store the R2 score
Matric_xgb = evaluate_regression_model(xgb_model, X_normalized_train, y_normalized_train,

# Print the R2 score
print(f"R-Square: {Matric_xgb}")

```

```

R-Square 0.9888518761408048

```

Figure 3.6: Extreme Gradient Boost prediction model code

### 3.9.1 Decision Trees (DT)

The DT approach is often used for tasks that require both regression and categorization. DT algorithm divides the results of the input parameters into subsets and labels are assigned to each subset according to the majority class (Suthaharan et al. 2016). The resulting tree structure can be used to make predictions on new data by traversing the tree from the starting point to a leaf node that correlates with a specific class or value. Quinlan asserts that decision trees are particularly useful in scenarios containing discrete-valued output parameters because they can manage both continuous and categorized input features. They are a popular option for exploratory data analysis and decision-making activities since they are also simple to understand and depict. The software offers ranges of DT hyper parameters that may be adjusted using search for grids or Bayesian optimization, such as complexity parameters, the maximum number of trees, the minimum number and splits, etc. Numerous geotechnical applications, such as categorization and soil parameter prediction, have made use of DT algorithms.

```
[ ] # Create a classifier
    decision_tree_model = DecisionTreeRegressor(max_depth=5,min_samples_leaf=1,max_features=0.7)
    # Evaluate the classifier using the function
    r2_score_result1 = evaluate_regression_model(decision_tree_model, X_normalized_train, y_normalized_train,

    print(f"R-Square: {r2_score_result1}")

R-Square 0.9873438681175709
```

Figure 3.7: Decision Tree prediction model code

### 3.10 Artificial Neural Network (ANN)

ANN is a modeling approach that permits learning by instance from data that is representative that explains a physical phenomenon or a decision-making process. It is inspired by the human being's nervous system. The ability of ANN to extract sophisticated knowledge and delicate information from representative data sets, as well as to build empirical correlations between variables that are both independent and dependent, is one of its distinctive features (Talwar, 2022). It is possible to establish the links between dependent and independent variables without making any presumptions

regarding the phenomenon's mathematical representation. ANN models provide several benefits over regression-based models, such as the ability to handle noisy data.

$$y = w_1x_1 + w_2x_2 + w_3x_3 + bias \quad (1)$$

$$y = \sum_{i=1}^n (w_i * x_i) + b \quad (2)$$

$$z = \frac{1}{1 + e^{-(w_1x_1 + w_2x_2 + w_3x_3 + b)}} \quad (3)$$

```

model = keras.Sequential([
    keras.layers.Dense(64, activation='relu', input_shape=(X_normalized_train.shape[1],)),
    keras.layers.Dense(32, activation='relu'),
    keras.layers.Dense(16, activation='relu'),
    keras.layers.Dense(8, activation='relu'),
    keras.layers.Dense(1) # Output layer for regression
])
model.compile(optimizer='adam', loss='mean_squared_error', metrics=['mean_absolute_error'])
history = model.fit(X_normalized_train, y_normalized_train, epochs=100, batch_size=32, validation_data=(X_normalized_test,
loss, mae = model.evaluate(X_normalized_test, y_normalized_test)
print(f"Test Loss: {loss}")
print(f"Mean Absolute Error (MAE): {mae}")
y_pred_ann = model.predict(X_normalized_test)

```

Figure 3.8: ANN prediction model code

### 3.11 Performance Evaluation:

A variety of metrics were used to evaluate the suggested model's performance indices, such as  $R^2$ , RMSE, MAE, NSE, Weighted Index, and Percent Bias. The performance indices' mathematical formulation is in equations given below. Table 2 displays these performance indexes' optimal values.

$$MAE = \frac{1}{n} \sum_{i=0}^{n-1} (|y_i - x_i|) \quad (4)$$

$$R^2 = 1 - \frac{\sum (y_i - \hat{y})^2}{\sum (y - y_i)^2} \quad (5)$$

$$NSE = 1 - \frac{\sum_{i=1}^n Q_{oi} - Q_{si}^2}{\sum_{i=1}^n Q_{oi} - \mu_o^2} \quad (6)$$

$$MSE = \sqrt{\frac{\sum_{i=1}^n (x_i - y_i)}{n}} \quad (7)$$

$\Sigma$ : Summation of all values

yi: Actual value for the i<sup>th</sup> observation

xi: Calculated value for the i<sup>th</sup> observation

N: Total number of observations

$$WI = \left[ 1 - \frac{\sum_{i=1}^n (d_i - y_i)^2}{\sum_{i=1}^n \{|y_i - d_{avg}| + |d_i - d_{avg}|\}^2} \right] \quad (8)$$

Where  $y_i$  is the model's anticipated probability of the liquefied value,  $d_{avg}$  denotes the mean value of  $d_i$ , and  $n$  denotes the total number of data points in that specific phase. Where  $d_i$  represents the actual likelihood of the liquefaction value.

$$PBIAS = \frac{\sum_{i=1}^n (Y_i^{obs} - Y_i^{sim})}{\sum_{i=1}^n (Y_i^{obs})} \quad (12)$$

## Chapter 4: Results and discussion

### 4.1 Preprocessed data

This study focused on determining the dynamic properties and liquefaction potential of soil by considering the shear stress, shear wave velocity and maximum shear modulus by utilizing machine learning techniques. In this section, the performance of the proposed models has been evaluated and discussed. Moreover, the model's performance has also been compared to identify the best model for prediction of liquefaction properties. It includes soil parameters analysis to evaluate the role of investigated parameters in determining the dynamics and liquefaction potential of soil, graphical representation of actual and predicted values of parameters for model's performance, Performance analysis, Accuracy matrix, AIC criteria and Comparative analysis.

#### 4.1.1 Soil Parameters Analysis

The sub-surface soil investigation clearly exhibited the contributing role of soil parameters in determination of dynamic properties and liquefaction potential of soil. The accurate assessment of shear stress is beneficial in grasping the soil behavior under dynamic load or seismic events. The significant cyclic stress during earthquakes caused contact loss and rearrangement of soil particles, leading to decrease in shear strength make them prone to liquefaction. Shear stress has a crucial role in determining the dynamic characteristics of soil, including damping ratio and shear modulus. Shear stress is a key parameter that numerical models primarily employ to simulate soil behavior under dynamic loading conditions. Precise modelling of shear stress is necessary to obtain accurate predictions of soil response (Yang et al. 2022). The stiffness and elastic characteristics of the soil are directly correlated with shear wave velocity. Usually, greater shear wave velocities signify more elastic and rigid soils. It is an important factor in determining the susceptibility of soil to liquefaction during seismic conditions. Low shear wave velocities are frequently linked to saturated, loose soils that are liquefiable (Aytas et al. 2023) Shear wave velocity is an essential input variable for response evaluation since it helps to predict how a particular site will react to seismic stresses. Maximum shear modulus is a key contributing factor in assessing the stiffness and shear strength of soil in response to dynamic loading circumstances.  $G_{max}$  refers to the soil's maximal stiffness. When dynamic stresses are applied, stiffer soil typically shows less setting and deformation. It is a typical dynamic property, and its lower value is associated with the higher risk

of liquefaction because dynamic loading can cause the soil to deform excessively and lose its strength. Maximum shear modulus is directly correlated with shear velocity. Therefore, it is the most essential input parameter for forecasting the dynamic behavior of soil under seismic load. Moreover, the pore water pressure and damping ratio has also the contributing role in evaluating the soil properties as the excessive PWP resulted in the reduction in stiffness and stability of soil and hence resulted in decrease in the shear strength, shear wave velocity and maximum shear modulus. Greater PWP is the primary indicator of liquefaction potential of soil. The results of the seismic response and DEEPSOIL analysis indicated that these parameters have the potential role in evaluating the dynamic properties and liquefaction potential of soil.

#### **4.1.2 Graphical Representation of Actual and Predicted Values**

This section graphically displays the performance of all the suggested models including KNN, FR, GB, XGBoost, DT and ANN as scatter plot of the actual and predicted probability values of the determined parameters (Shear stress, shear wave velocity and maximum shear modulus). Scatter plot from machine learning algorithms comparing the actual against anticipated probability is a valuable diagnostic tool for assessing the performance and accuracy of predictive models. Predicted probabilities that accurately reflect the possibility of an occurrence should be generated using a well-calibrated model. The scatter plot data points in this instance should be dispersed evenly around the 45o line. The models show better prediction accuracy when the plotted data points fall closer to the line ( $x = y$ ) which means that the predicted values are close to the actual. The deviation from the line indicated that the predicted probability is not accurately representing the true possibilities. Points above the line indicated the overestimation and data points below the line indicated the underestimation. A tight cluster of points around the line demonstrates consistency, whereas the dispersed distribution indicated variability in prediction. The scatter graphs display for each of the parameters predicted by various machine learning models are given and discussed below.

#### **4.1.3 Shear Stress**

The scatter plots of actual and predicted shear stress data are given in figure 3 below. It can be seen from the plots that all the models have shown reasonable performance in terms of shear stress prediction. Figure 3b from random forest (RF) model indicated the least scattering from the line and the predicted datapoints are closer to the actual ones demonstrating the highest efficiency of

all the suggested models for shear stress evaluation. Figure 3d of XGBoost also demonstrated the higher performance for SS prediction as this graph shows limited number of scatter values after RF. The efficiency of remaining models for the prediction of shear stress for liquefaction potential identification is in the order of DT > GB > ANN > KNN. Both ANN followed by KNN models showed the variant predicted data points from the actual data and least efficacy for shear stress evaluation from the input parameters. The coefficient of determination has also been evaluated from the scatter graphs for the numerical analysis of all the model's performance and are given in next section.



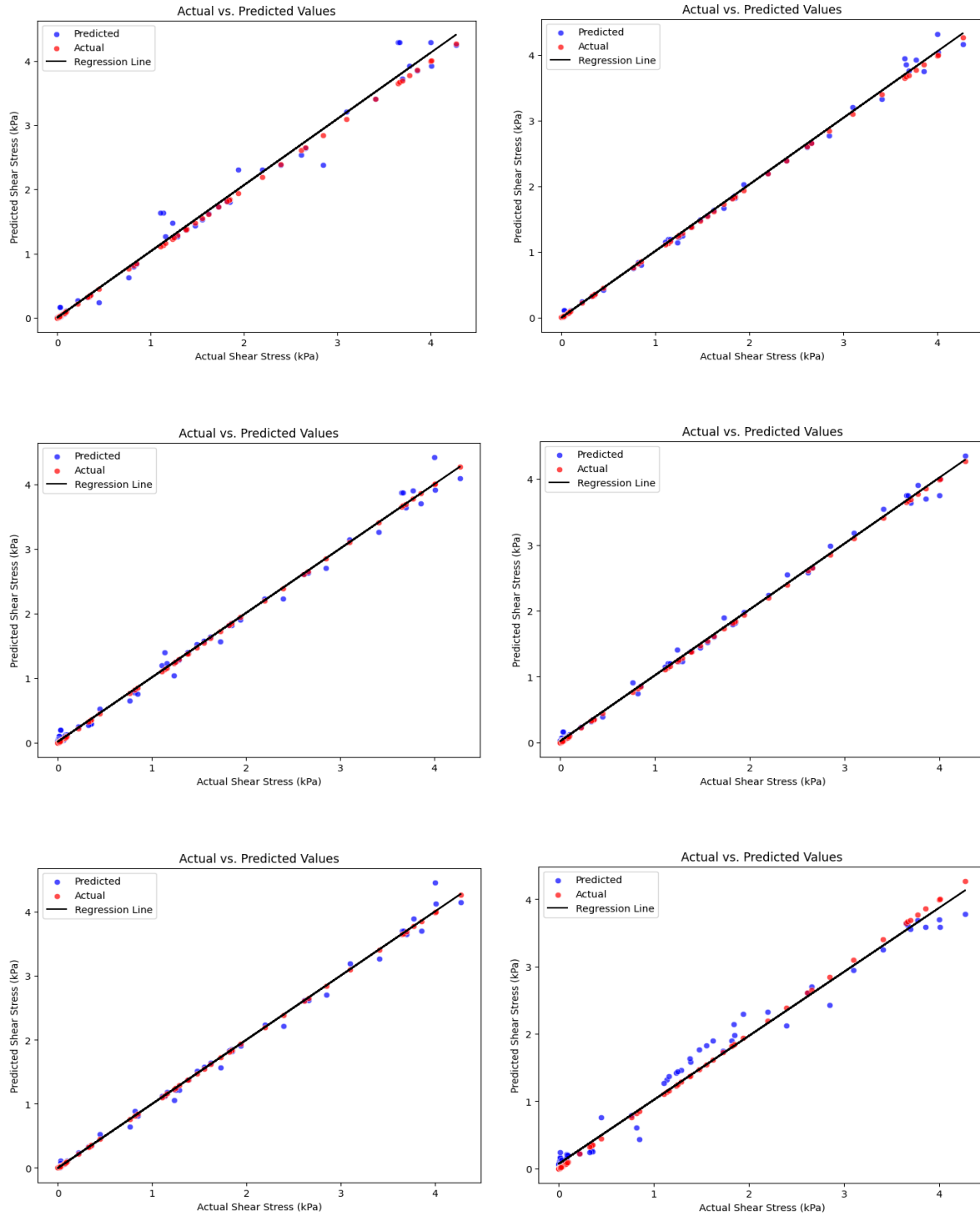


Figure 4.1 : Scatter graphs for shear stress prediction: (a) KNN, (b) RF, (c) GB, (d) XGBoost, (e) DT and (f) ANN

#### 4.1.4 Shear wave Velocity

The scatter plots of actual and predicted data of shear wave velocity are given in figure 4 below. The plots of all the models have been assessed to evaluate their performance for shear wave velocity prediction. The graphs in figure 4 indicated that all the models have slight greater variation in prediction and actual value of shear wave velocity than the other parameters. GB model in figure 4c has the least scatter predicted values than the other models. Gradient boost exhibited the best performance for determining the shear wave velocity. Moreover, RF in figure 4b also indicated better performance as compared to the other models. SV prediction efficiency by the proposed models is in order of  $GB > RF > KNN > ANN > XGBoost > DT$ . Decision tree model has indicated the minimum performance for shear velocity evaluation in liquefaction potential determination.

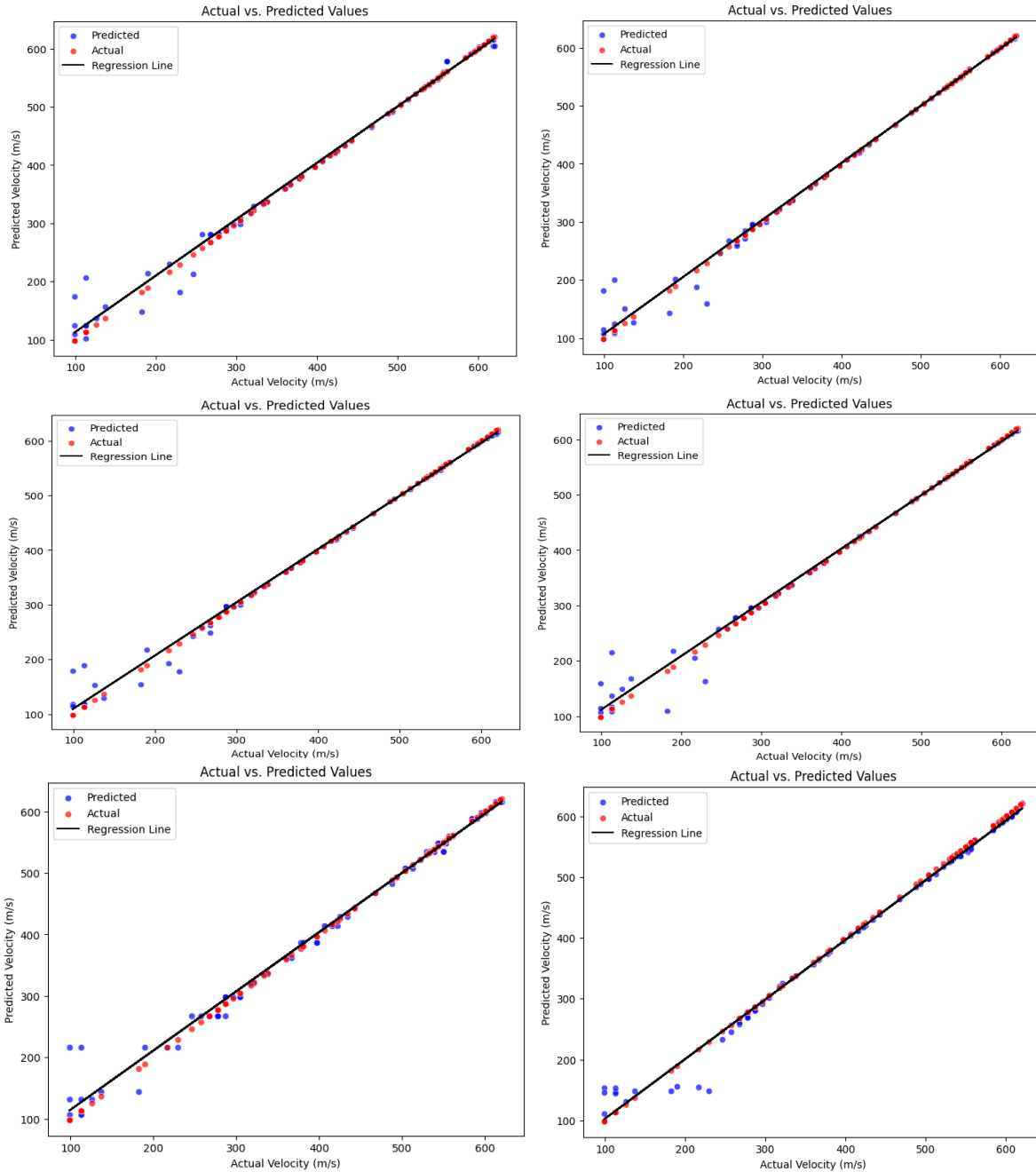


Figure 4.2: Scatter graphs for shear wave velocity prediction: (a) KNN, (b) RF, (c) GB, (d) XGBoost, (e) DT and (f) ANN

## 4.2 Maximum Shear Modulus

The scatter graphs of Gmax actual and predicted data by various suggested models is given in figure 5 below. The graphs indicated the evenly distributed datapoints with predicted value closer to the line or actual values. The less scattering of datapoints in the graph exhibited the well-

calibrated models for Gmax prediction. It can be seen from graphs that these models have highest efficiency for Gmax prediction than other parameters to evaluate the dynamic properties and liquefaction potential. Figure 5d of ANN model exhibited the highest performance efficiency for maximum shear modulus prediction as this graph indicated least scattering from the actual data. Decision tree (DT) model (5e) also indicated greater efficiency with very little predicted data variability. KNN model in 5a has limited efficacy for Gmax as compared to all other models. The trend for Gmax prediction from the input parameters of all models is in order of ANN > DT > XGBoost > RF > GB > KNN. As liquefaction potential is highly dependent on maximum shear modulus, Gmax prediction is extremely useful for assessing the dynamic properties of soil.

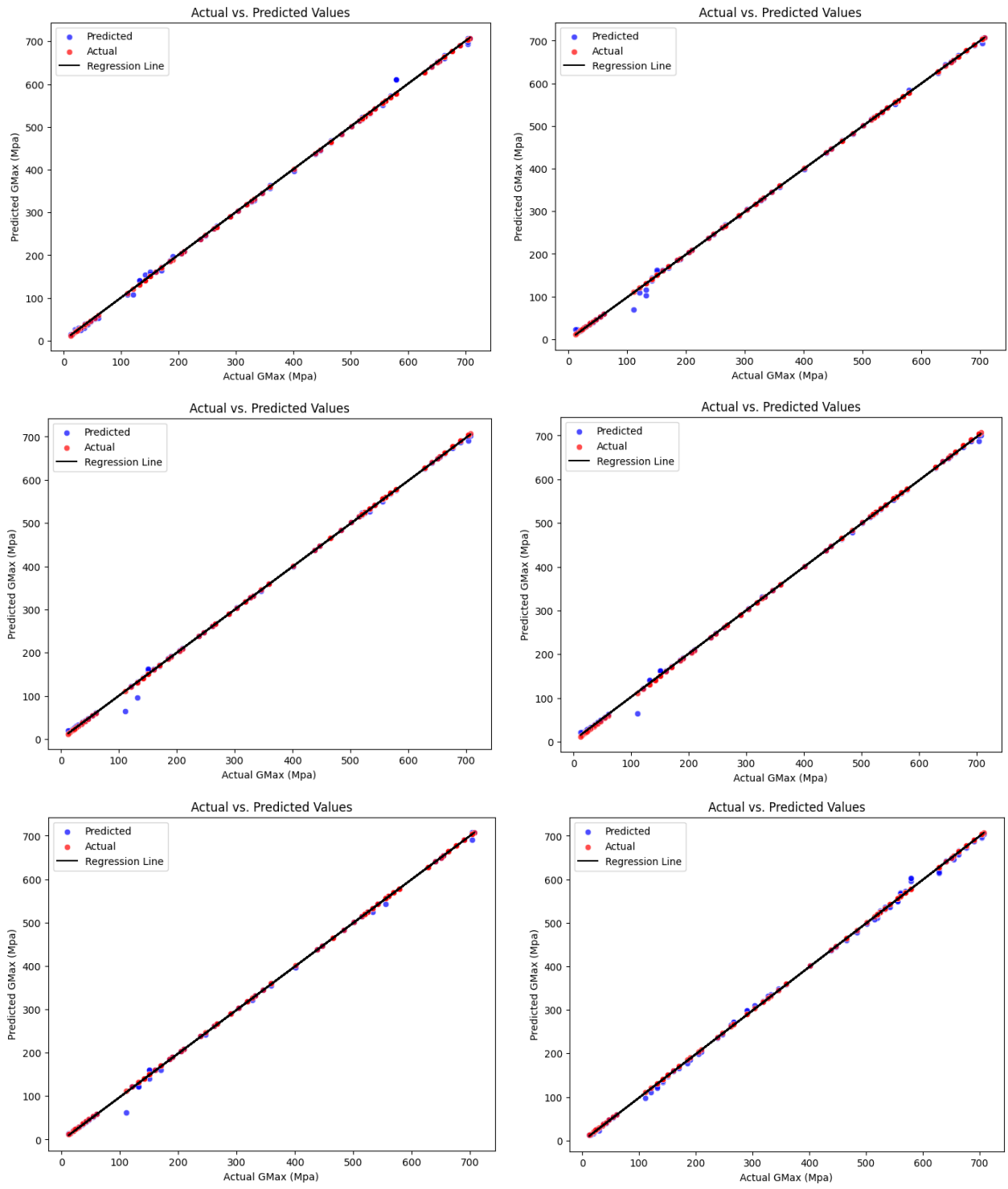


Figure 4.3: Scatter graphs for shear wave velocity prediction: (a) KNN, (b) RF, (c) GB, (d) XGBoost, (e) DT and (f) ANN

### 4.3 Liquefaction Potential Index

The scatter plots for LIP prediction of all the proposed models are given in Figure 6 below. It can be clearly seen from the graphs that all models showed satisfactory performance for LIP determination when predicted by using the other soil parameters. XGBoost model outperformed all the models predicting LIP as there is comparatively less scattering of predicted values from the actual data as shown in Figure 6d. Moreover, DT model also exhibited greater efficiency in this parameter determination and almost have relatable performance to XGBoost model (Figure 6e). The highest scattering from the predicted data and in turn the least performance is observed in case of KNN model (Figure 6a). The general trend for the determination of LIP of soil by considering all other parameters is in the order of XGBoost > DT > RF > GB > ANN > KNN. The various performance indices have also been calculated from the plots and are discussed in the next section.

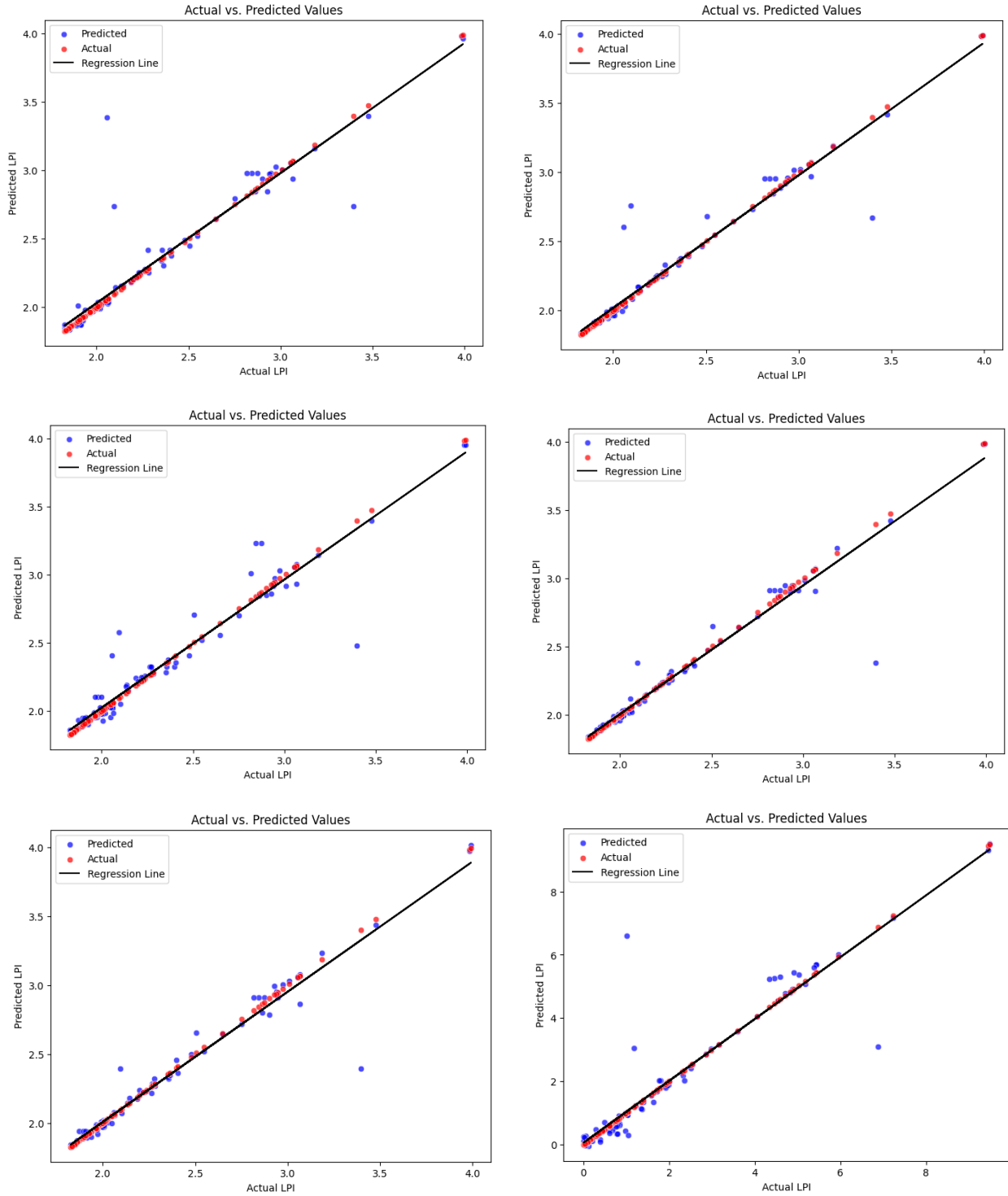


Figure 4.4: Scatter graphs for LIP prediction: (a) KNN, (b) RF, (c) GB, (d) XGBoost, (e) DT and (f) ANN

#### 4.4 Performance analysis

The performance of the recommended models (KNN, RF, GB, XGBoost, DT and ANN) has been computed with the help of various evaluation matrices. Consequently, the real and anticipated probability values of various parameters (SS, SV, Gmax, LIP) has been utilized to evaluate the performance indices. The real values of the calculated evaluation indices used for the performance analysis is given in table 3 below. It can be seen from the table that for shear stress determination, RF indicated lower efficiency errors with high 0.998 Nash-Sutcliffe Efficiency and 0.998 coefficient of determination  $R^2$ . High R-squared value close to 1 indicated that this model regarded as good and optimized model for shear stress prediction. By determining the SS values, we can evaluate the dynamic properties and liquefaction potential of soil. Similarly, for SV prediction, gradient boost (GB) model performed best with less efficiency errors, 0.990 of Nash-Sutcliffe Efficiency and 0.992 coefficient of determination. By examining the SV, we can easily determine the trend of liquefaction potential of soil. Furthermore, maximum shear modulus (Gmax) considered as the highest contributing parameter in assessing the liquefaction potential. ANN model indicated the best performance efficiency for Gmax prediction with 0.999 Nash-Sutcliffe Efficiency and 0.999  $R^2$ . LIP of soil has also been determined with greater  $R^2$  value of 0.946 and NSE of 0.904 by XGBoost model. This indicated that these model are highly optimized model for Gmax and LIP determination.

Table 4.1: Performance Matrices values for all models

Parameters	Evaluation Indices	Models					
		KNN	RF	GB	XGBoost	DT	ANN
SS	MSE	0.020	0.004	0.007	0.004	0.005	0.014
	RMSE	0.142	0.060	0.085	0.061	0.070	0.120
	MAE	0.054	0.025	0.050	0.038	0.031	0.075
	Nash-Sutcliffe Efficiency	0.987	0.998	0.995	0.998	0.997	0.990
	Percent Bias	3.599	1.201	1.542	2.615	0.193	3.083

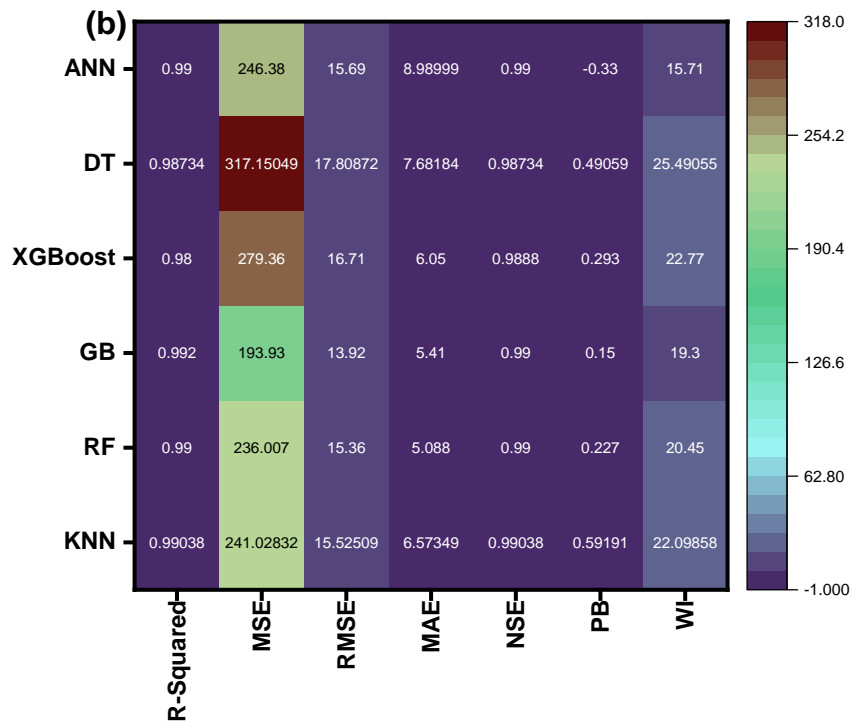
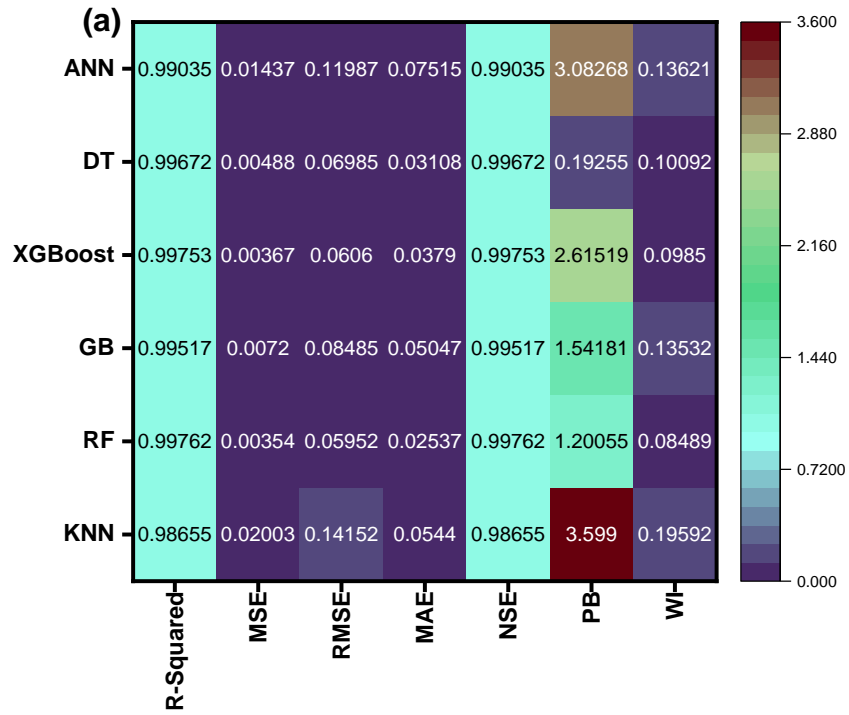


	Weighted Index	0.196	0.085	0.135	0.098	0.101	0.136
	R <sup>2</sup>	0.987	<b>0.998</b>	0.995	0.998	0.997	0.990
<b>SV</b>	MSE	241.028	236.007	193.930	279.360	317.150	246.380
	RSME	15.525	15.360	13.920	16.710	17.809	15.690
	MAE	6.573	5.088	5.410	6.050	7.682	8.990
	Nash-Sutcliffe Efficiency	0.990	0.990	0.990	0.989	0.987	0.990
	Percent Bias	0.592	0.227	0.150	0.293	0.491	-0.330
	Weighted Index	22.099	20.450	19.300	22.770	25.491	15.710
	R <sup>2</sup>	0.990	0.990	<b>0.992</b>	0.980	0.987	0.990
<b>Gmax</b>	MSE	45.731	36.084	43.090	35.920	35.333	34.840
	RMSE	6.762	6.007	6.560	5.993	5.944	5.900
	MAE	3.134	2.337	2.672	2.789	1.829	4.612
	Nash-Sutcliffe Efficiency	0.999	0.999	0.999	0.999	0.999	0.999
	Weighted Index	0.281	-0.190	-0.230	-0.080	-0.297	-0.050
	Percent Bias	9.897	8.344	9.230	8.783	7.773	5.900
	R <sup>2</sup>	0.999	0.999	0.999	0.999	0.999	<b>0.9999</b>
<b>LPI</b>	MSE	0.0278	0.0137	0.0175	0.0121	0.0124	0.0242
	RMSE	0.167	0.117	0.1324	0.1101	0.111	0.736
	MAE	0.050	0.035	0.061	0.032	0.035	0.0256

Nash-Sutcliffe Efficiency	0.872	0.939	0.932	0.904	0.945	0.876
Weighted Index	0.217	0.153	0.193	0.142	0.147	0.850
Percent Bias	0.781	0.352	0.443	0.352	0.326	0.143
R <sup>2</sup>	0.877	0.939	0.922	<b>0.946</b>	0.945	0.875

**4.4.1 Accuracy Matrix**

Heatmaps of the evaluation matrix statistical data are presented in figure 7. Heatmaps are created to present and visualize complex data and to identify the trends, patterns and variations. With color variations, the heatmap matrix shows the statistical parameter values and makes it easier to examine the multivariate data produced by different models’ side by side. The generation of heatmap is based on the comparison of model’s ideal values of the statistical parameters obtained from the predicted parameter values. The heatmap of shear stress in figure 7a indicated the color variation between the higher performed model RF and less performed model ANN and KNN. The difference in intensity of colors of various parameters indicates the trend of models for prediction efficiency performance. Similarly, the higher intensity colors of XGboost and DT in 7b indicated the least performance for SV prediction. The correlation pattern and trend of performance in figure 7c is exhibited by color variation and showed ANN as best model and DT and XGboost as least performing models for maximum shear modulus prediction. The accuracy matrix of LIP parameter also indicates the higher zones along the three models (GB, ANN and KNN) which exhibited less efficiency as compared to all other three models.



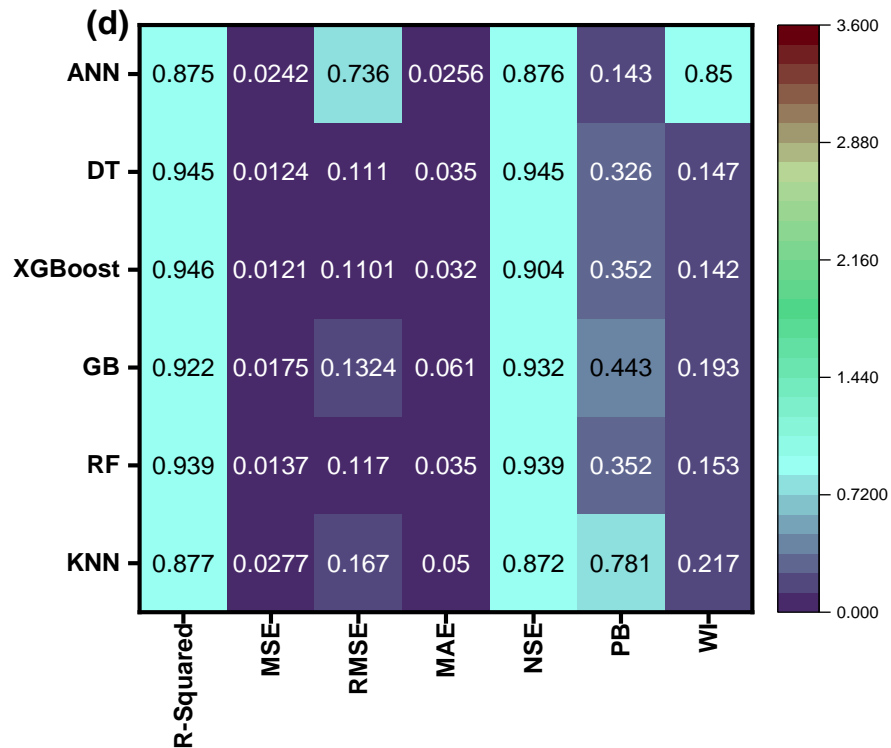
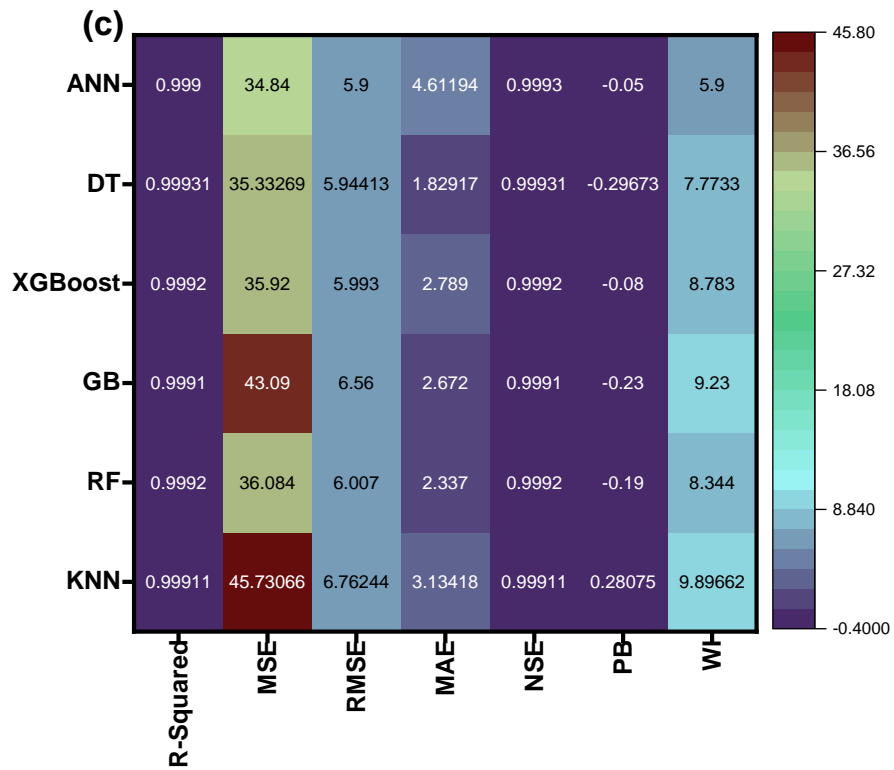


Figure 4.5: Accuracy Matrix of statistical parameters data (a) SS (b) SV (c) Gmax (d) LPI

#### 4.4.2 AIC Criteria

Akaike Information Criteria (AIC) is a statistical metric employed to choose model and assess their generalization (Akaike, 2011). The AIC offers a quantitative method for comparing several models and determining which strikes the optimal trade-off between model complexity and goodness of fit. The following is the mathematical expression that was used to determine the AIC value:

$$AIC = n \times \ln(RSME^2) + 2k \quad (9)$$

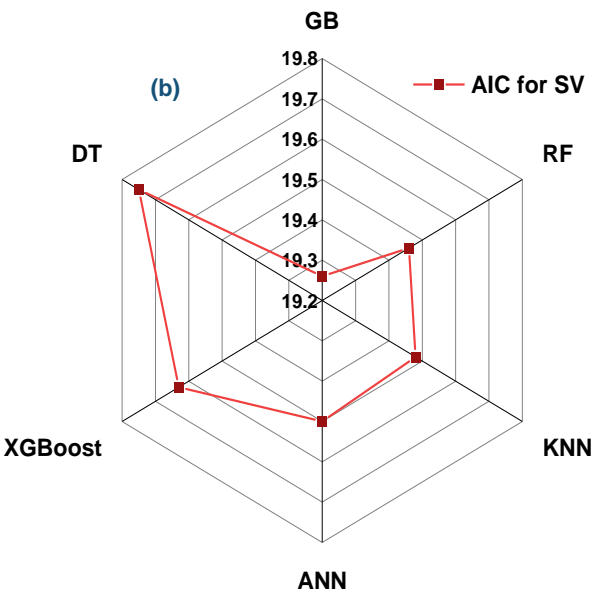
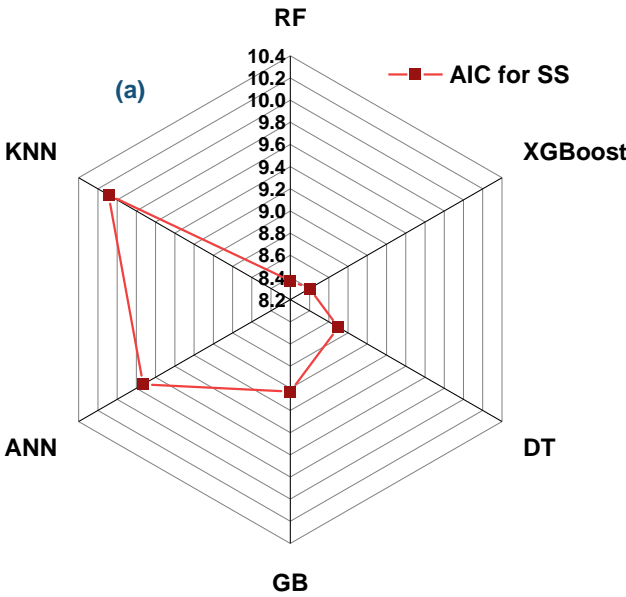
In this equation,  $n$  represents the dependent variable,  $RSME$  is determined by the actual and predicted data,  $2k$  indicates the maximum number of independent variables that are utilized in the models. The term  $n \times \ln(RMSE^2)$  indicates goodness of fit model.

The model with lowest AIC value when compared with the other ones regarded as the best-fitted model for the data. The model that fits the data the best when compared to other models is the one with the lowest AIC value. By opting for the model with the lowest AIC, researchers can strike a compromise between model intricacy and goodness of fit, favouring more straightforward models that nonetheless provide a sufficient explanation for the data. Remember that the AIC is a comparison metric and does not offer a precise assessment of model fit. Its main application is to compare models within a given dataset. The AIC values for each model for various parameter prediction is given in table 4 below. The calculated AIC values are in accordance with the evaluation matrices. RF model has the lowest AIC value of 8.37 for shear stress prediction than all other models. This also indicates that RF model has highest efficiency for SS evaluation. Similarly, GB and ANN model has lowest AIC values of 19.26 and 17.55 for shear wave velocity and maximum shear modulus prediction respectively. The values of AIC for LPI parameter are also in accordance with the above findings and lowest AIC value of 9.58 is indicated by XGBoost model. These models with lowest AIC values indicate the goodness of fit model. Furthermore, all other AIC values also follow the performance trend for all four parameters. The decreasing trends of models performance by increasing AIC values for shear stress, shear wave velocity, maximum shear modulus and LPI in the form of radar diagrams are shown in figure 8 below.

Table 4.2 AIC values of parameters for all proposed models

Models	Parameters
--------	------------

	SS	SV	Gmax	LIP
KNN	10.09	19.48	17.82	10.41
RF	8.37	19.46	17.58	9.71
GB	9.03	19.26	17.76	9.95
XGBoost	8.40	19.63	17.58	9.58
DT	8.7	19.75	17.56	9.6
ANN	9.73	19.50	17.55	10.28



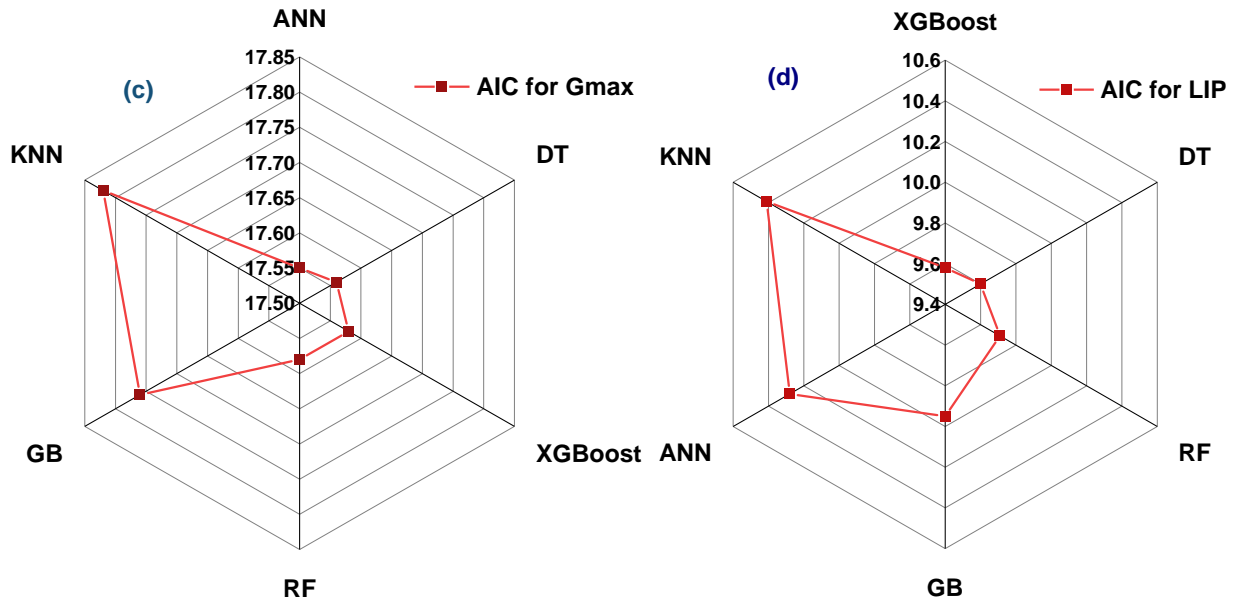


Figure 4.6: Illustration of all proposed Model's AIC values using Radar Diagram for (a) SS parameter (b) SV parameter (c) Gmax parameter

#### 4.5 Rank Analysis

Rank analysis is carried out to overall compare the model's performance for determination of liquefaction potential. Rank analysis is conducted based on the model's efficiency in predicting the parameters. This analysis entails score assigning to each model based on their optimized performance for prediction. In this analysis, 1 to 6 score is assigned to each model for each parameter prediction (SS, SV, Gmax) with lowest score (1) exhibiting the highest efficiency and the highest score (6) indicated the indeterminacy or less efficiency of model. In this way, score is assigned to each model for all the three parameters separately and then add the scores of each parameter of all individual models. The model with lowest final score is positioned as first in the rank for the overall determination of liquefaction potential while the suggested model with highest total score holds the last rank for prediction efficiency. The ranks or scores of various models for assessing the parameters and the final total score is given in table 4 below. The table indicated that random forest (RF) model exhibited the lowest total score and ranked first with highest performance for liquefaction potential determination. This indicated that RF has proved to be the most efficient model for all types of parameter prediction. Next XGBoost and DT indicated greater performance after RF model. These models performed either good or less effectively for different parameters. GB model ranked fourth while KNN model has highest score of 21 or least ranking in

performance efficiency. The KNN model proved to be least suitable for liquefaction potential assessment of soil.

Table 4.3: Ranking analysis of all models for dynamic properties and liquefaction potential determination

Parameters	Models					
	KNN	RF	GB	XGBoost	DT	ANN
<b>SS</b>	6	1	4	2	3	5
<b>SV</b>	3	2	1	5	6	4
<b>Gmax</b>	6	4	5	3	2	1
<b>LIP</b>	6	3	4	1	2	5
<b>Total score</b>	<b>21</b>	<b>10</b>	<b>14</b>	<b>11</b>	<b>13</b>	<b>15</b>
<b>Rank</b>	<b>6<sup>th</sup></b>	<b>1st</b>	<b>4th</b>	<b>2<sup>nd</sup></b>	<b>3rd</b>	<b>5th</b>



## Chapter 5: Conclusions

In conclusion, the use of ML algorithms has proven to be a useful and promising strategy in assessing the dynamic properties and liquefaction potential of soil. Six regression models including KNN, RF, GB, XGBoost, DT and ANN improved our vision of understanding soil behavior under seismic conditions by employing the large input SPT-N dataset of soil parameters. This paper includes a detailed evaluation of dynamic characteristics such as SS, SV, Gmax and LPI that are crucial in comprehending the behavior of soil during seismic events. The assessment of liquefaction potential is also conducted which is a crucial element in determining earthquake vulnerability. By employing the unique benefits of several machine learning approaches, this research aims to construct robust and accurate models capable of predicting soil responses and liquefaction susceptibility. The performance of the models has been evaluated by using the evaluation indices of MSE, RMSE, MAE, Nash-Sutcliffe Efficiency, Percent Bias, Weighted Index and R-squared. The model's analysis has been conducted by scatter diagram, evaluation indices, Accuracy matrix, AIC criteria and Ranking Analysis. Following are the results obtained from this assessment.

- It has been found that RF model performed well for shear stress prediction with  $R^2$  of 0.998, RMSE of 0.060 and NSE of 0.998. Its Scatter diagram indicated the least scattering from the actual values. AIC criteria also indicated its highest efficiency with lowest AIC value in SS prediction. XGBoost also indicated nearly the same efficiency with RMSE of 0.061 and considered the second best prediction model for SS. Next the performance trend is followed by DT > GB > ANN > KNN.
- For Shear Wave velocity prediction, GB was found to be the best model with 0.992 R-squared value, 0.990 NSE and 13.920 RMSE. Accuracy matrix and AIC criteria also exhibited its highest efficiency followed by RF > KNN > ANN > XGBoost > DT for SV prediction from SPT-N dataset.
- The performance analysis of models for maximum shear modulus ranked ANN model on the top for Gmax forecasting with 0.999  $R^2$  value, 0.99 NSE and 0.56 RMSE. All other models also performed well for Gmax prediction which is a most important parameter for liquefaction determination. The performance trend is in the order of ANN > DT > XGBoost > RF > GB > KNN.

- For LPI parameter, XGBoost and DT models found to be the best predicting models for evaluating the liquefaction potential of soil. These models exhibited lower error for determination along with 0.946 R-squared value and only 0.352 and 0.142 PB and WI respectively. The general trend of models for LPI prediction in as: XGBoost > DT > RF > GB > ANN > KNN.
- For comparative analysis of models, the scaling analysis is conducted, and score is assigned to each model according to their performance number. This analysis indicated that RF model ranked first for overall dynamic properties and liquefaction potential prediction with lowest score of 10. Moreover, XGBoost (11) and DT (13) found to be the second and third highest optimized models respectively for liquefaction potential determination. GB is assigned with total score of 14 and served on fourth rank while ANN and KNN showed the least performance with 15 and 21 rank score respectively.

The detailed analysis of this work demonstrates how machine learning may be used to capture intricate relationships between various input parameters and the dynamic response of soil. The algorithms showed unique skills to handle complex, nonlinear patterns found in geotechnical data. It contributes to the growing body of information in geotechnical engineering and its findings have relevance for infrastructure design and seismic risk assessment. The developed machine learning models have major applications for geologists and architects as they provide a dependable means of predicting and mitigating soil liquefaction hazards. The variety of scenarios in which machine learning models can be used to soil dynamics may be expanded and improved by further research in this field. More datasets, enhanced feature engineering techniques, and more intricate model designs can all help improve the reliability and robustness of predictive models. Ultimately, the integration of artificial intelligence into geotechnical processes represents a significant breakthrough in our ability to design resilient infrastructure and structures that can withstand the challenges posed by seismic activity and soil liquefaction.

## References

Akaike, H. (2011). Akaike's information criterion. *International encyclopedia of statistical science*, 25-25.

A. Ansari, F. Zahoor, K. Sehasgiri Rao & A. Kumar Jain (2022) Liquefaction hazard assessment in a seismically active region of Himalayas using geotechnical and geophysical investigations: a case study of the Jammu Region *Bulletin of Engineering Geology and the Environment* (2022) 81: 349 <https://doi.org/10.1007/s10064-022-02852-3>

Aytaş, Z., N. Alpaslan, and F. Özçep, Evaluation of liquefaction potential by standard penetration test and shear wave velocity methods: a case study. *Natural Hazards*, 2023. 118(3): p. 2377-2417.

Ali SM, Khan AN, Rahman S, Reinhorn AM. A Survey of Damages to Bridges in Pakistan after the Major Earthquake of 8 October 2005. *Earthquake Spectra*. 2011;27(4):947-970. doi:10.1193/1.3650477.

Amroune, M. (2022). Support vector regression-bald eagle search optimizer-based hybrid approach for short-term wind power forecasting. *Journal of Engineering and Applied Science*, 69(1), 107.

Arboleda-Monsalve, L. G., Mercado, J. A., Terzic, V., & Mackie, K. R. (2020). Soil–structure interaction effects on seismic performance and earthquake-induced losses in tall buildings. *Journal of Geotechnical and Geoenvironmental Engineering*, 146(5), 04020028.

Ayala, F., Sáez, E., & Magna-Verdugo, C. (2022). Computational modelling of dynamic soil-structure interaction in shear wall buildings with basements in medium stiffness sandy soils using a subdomain spectral element approach calibrated by micro-vibrations. *Engineering Structures*, 252, 113668.

Bhalawe, S., Nayak, D., Lodhi, A., Thakur, R., Rai, S., & Shrivastava, A. (2024). Soil Dynamics for Carbon Buildup in Different Land Use Systems in the South Region of Gujarat, India. *Journal of Experimental Agriculture International*, 46(1), 77-86.

Cai, Mingxiang & Ouaer, Hocine & Mohammed, Ahmed & Chen, Xiaoling & Nait Amar, Menad & Hasanipanah, Mahdi. (2022). Integrating the LSSVM and RBFNN models with three optimization algorithms to predict the soil liquefaction potential. *Engineering with Computers*. 38. 1-13. [10.1007/s00366-021-01392-w](https://doi.org/10.1007/s00366-021-01392-w).

Chen, T. and C. Guestrin. Xgboost: A scalable tree boosting system. in Proceedings of the 22nd acm sigkdd international conference on knowledge discovery and data mining. 2016.

Das, S. K., & Muduli, P. K. (2011). Evaluation of liquefaction potential of soil using genetic programming. Paper presented at the Proceedings of the golden jubilee indian geotechnical conference, Kochi, India.

Erzin, Y., & Tuskan, Y. (2019). The use of neural networks for predicting the factor of safety of soil against liquefaction. *Scientia Iranica*, 26(5), 2615-2623.

Fahim, A. K. F., Rahman, M. Z., Hossain, M. S., & Kamal, A. M. (2022). Liquefaction resistance evaluation of soils using artificial neural network for Dhaka City, Bangladesh. *Natural Hazards*, 113(2), 933-963.

Forte, G., Chioccarelli, E., De Falco, M., Cito, P., Santo, A., & Iervolino, I. (2019). Seismic soil classification of Italy based on surface geology and shear-wave velocity measurements. *Soil Dynamics and Earthquake Engineering*, 122, 79-93.

GASHAW, H. (2020). ASSESSMENT AND EVALUATION OF EARTHQUAKE-INDUCED SOIL LIQUEFACTION POTENTIAL: A CASE STUDY IN HAWASSA TOWN. *ARCHITECTURAL ENGINEERING*,

Ghani, S., & Kumari, S. (2022). Liquefaction behavior of Indo-Gangetic region using novel metaheuristic optimization algorithms coupled with artificial neural network. *Natural Hazards*, 111(3), 2995-3029.

Guo, H., Zhuang, X., Chen, J., & Zhu, H. (2022). Predicting earthquake-induced soil liquefaction based on machine learning classifiers: A comparative multi-dataset study. *International Journal of Computational Methods*, 19(08), 2142004.

Hanandeh, Shadi & Al-Bodour, Wassel & Hajj, Mustafa. (2022). 3 A Comparative Study of Soil Liquefaction Assessment Using Machine Learning Models. *Geotechnical and Geological Engineering*. 40. 10.1007/s10706-022-02180-z

Hossain, M. B., Roknuzzaman, M., & Rahman, M. M. (2022). Liquefaction Potential Evaluation by Deterministic and Probabilistic Approaches. *Civil Engineering Journal*, 8(7), 1459-1481.

Huang, B., Chen, X., & Zhao, Y. (2015). A new index for evaluating liquefaction resistance of soil under combined cyclic shear stresses. *Engineering Geology*, 199, 125-139.

Ji, Y., Kim, B., & Kim, K. (2021). Evaluation of liquefaction potentials based on shear wave velocities in Pohang City, South Korea. *International Journal of Geo-Engineering*, 12, 1-10.

Kasim, M. N., & Raheem, A. M. (2021). Evaluation of some soil characteristics from field SPT values using random number generation technique. Paper presented at the IOP Conference series: earth and environmental science.

Kayabasi, A., & Gokceoglu, C. (2018). Liquefaction potential assessment of a region using different techniques (Tepebasi, Eskişehir, Turkey). *Engineering Geology*, 246, 139-161.

Khasawneh, M. A., Al-Akhrass, H. I., Rabab'ah, S. R., & Al-sugaier, A. O. (2024). Prediction of California bearing ratio using soil index properties by regression and machine-learning techniques. *International Journal of Pavement Research and Technology*, 17(2), 306-324.

Khan, M. Y., Saralioglu, E., Turab, S. A., & Muhammad, S. (2023). Tracking surface and subsurface deformation associated with groundwater dynamics following the 2019 Mirpur earthquake. *Geomatics, Natural Hazards and Risk*, 14(1). <https://doi.org/10.1080/19475705.2023.2195966>

Khan, Muhammad & Ali Turab, Syed & Riaz, Shahid & Atekwana, Estella & Muhammad, Said & Butt, Nabeel & Abbas, Syed & Zafar, Waqar & Ohenhen, Leonard. (2021). Investigation of coseismic liquefaction-induced ground deformation associated with the 2019 M w 5.8 Mirpur, Pakistan, earthquake using near-surface electrical resistivity tomography (ERT) and geological data. *Near Surface Geophysics*. 19. 10.1002/nsg.12148.

Kim, H.-S., Kim, M., Baise, L. G., & Kim, B. (2021). Local and regional evaluation of liquefaction potential index and liquefaction severity number for liquefaction-induced sand boils in Pohang, South Korea. *Soil Dynamics and Earthquake Engineering*, 141, 106459.

Kokusho, T. (2013). Liquefaction potential evaluations: energy-based method versus stress-based method. *Canadian Geotechnical Journal*, 50(10), 1088-1099.

Lu, C.-C., & Hwang, J.-H. (2020). Correlations between Vs and SPT-N by different borehole measurement methods: effect on seismic site classification. *Bulletin of Earthquake Engineering*, 18, 1139-1159.

Luque, R., & Bray, J. D. (2020). Dynamic soil-structure interaction analyses of two important structures affected by liquefaction during the Canterbury earthquake sequence. *Soil Dynamics and Earthquake Engineering*, 133, 106026.

Lusa, L., Gradient boosting for high-dimensional prediction of rare events. *Computational Statistics & Data Analysis*, 2017. 113: p. 19-37.

Maillo, J., et al., kNN-IS: An Iterative Spark-based design of the k-Nearest Neighbors classifier for big data. *Knowledge-Based Systems*, 2017. 117: p. 3-15.

- Mondal, J. K., & Kumar, A. (2024). New Frequency Domain Framework of Inverse Ground Response Analysis for the Determination of Dynamic Soil Properties of Multilayered System. *Indian Geotechnical Journal*, 54(2), 547-576.
- Mourlas, C., Khabele, N., Bark, H. A., Karamitros, D., Taddei, F., Markou, G., & Papadrakakis, M. (2020). Effect of soil–structure interaction on nonlinear dynamic response of reinforced concrete structures. *International Journal of Structural Stability and Dynamics*, 20(13), 2041013.
- Muduli, P. K., & Das, S. K. (2015). Evaluation of liquefaction potential of soil based on shear wave velocity using multi-gene genetic programming. *Handbook of genetic programming applications*, 309-343.
- Nejad, M. M., Momeni, M. S., & Manahiloh, K. N. (2018). Shear wave velocity and soil type microzonation using neural networks and geographic information system. *Soil Dynamics and Earthquake Engineering*, 104, 54-63.
- Ozsagir, M., Erden, C., Bol, E., Sert, S., & Özocak, A. (2022). Machine learning approaches for prediction of fine-grained soils liquefaction. *Computers and Geotechnics*, 152, 105014.
- Padarian, J., Minasny, B., & McBratney, A. B. (2020). Machine learning and soil sciences: A review aided by machine learning tools. *Soil*, 6(1), 35-52.
- Pakzad, A., & Arduino, P. (2024). Assessment of soil constitutive models for predicting seismic response of sheet pile walls: A LEAP-2022 project study. *Soil Dynamics and Earthquake Engineering*, 178, 108447.
- Pandey, A. and A. Jain, Comparative analysis of KNN algorithm using various normalization techniques. *International Journal of Computer Network and Information Security*, 2017. 11(11): p. 36.
- Richman, J.S., Multivariate neighborhood sample entropy: a method for data reduction and prediction of complex data, in *Methods in enzymology*. 2011, Elsevier. p. 397-408.
- Rigatti, S.J., Random forest. *Journal of Insurance Medicine*, 2017. 47(1): p. 31-39.
- Shahri, A. A., Behzadafshar, K., & Rajablou, R. (2013). Verification of a new method for evaluation of liquefaction potential analysis. *Arab J Geosci*, 6(3), 881-892.
- Si, S., et al. Gradient boosted decision trees for high dimensional sparse output. in *International conference on machine learning*. 2017. PMLR.
- Suthaharan, S. and S. Suthaharan, *Decision tree learning. Machine Learning Models and Algorithms for Big Data Classification: Thinking with Examples for Effective Learning*, 2016: p. 237-269.

Talwar, N. (2022). MODELING NON-LINEAR ASSOCIATIONS BETWEEN INDEPENDENT AND DEPENDENT VARIABLES USING ARTIFICIAL NEURAL NETWORKS IN PYTHON. *OORJA-International Journal of Management & IT*, 20(1).

Tran, D. T., Onjaipurn, T., Kumar, D. R., Chim-Oye, W., Keawsawasvong, S., & Jamsawang, P. (2024). An eXtreme Gradient Boosting prediction of uplift capacity factors for 3D rectangular anchors in natural clays. *Earth Science Informatics*, 1-15.

Yabe, H., Harada, K., Ito, T., & Watanabe, E. (2022). Study on SPT N-values and relative density through various soundings in full-scale chamber test ground. In *Cone Penetration Testing 2022* (pp. 772-777): CRC Press.

Yunmin, C., Han, K., & Ren-peng, C. (2005). Correlation of shear wave velocity with liquefaction resistance based on laboratory tests. *Soil Dynamics and Earthquake Engineering*, 25(6), 461-469.

Yang, J., L. Liang, and Y. Chen, Instability and liquefaction flow slide of granular soils: the role of initial shear stress. *Acta Geotechnica*, 2022. 17(1): p. 65-79.

Zeng, H., Tang, C.-S., Fraccica, A., Zhu, C., Tian, B.-g., & Shi, B. (2024). Multi-scale investigation on dynamic characteristics of clayey soil evaporation and cracking. *Computers and Geotechnics*, 171, 106312.

Zhang, P., Yin, Z.-Y., & Jin, Y.-F. (2022). Machine learning-based modelling of soil properties for geotechnical design: review, tool development and comparison. *Archives of Computational Methods in Engineering*, 1-17.

Zhao, Zening & Duan, Wei & Cai, Guojun. (2021). A novel PSO-KELM based soil liquefaction potential evaluation system using CPT and Vs measurements. *Soil Dynamics and Earthquake Engineering*. 150. 106930. 10.1016/j.soildyn.2021.106930.